Mechanically Controllable Break Junctions for Molecular Electronics

Dong Xiang, Hyunhak Jeong, Takhee Lee, and Dirk Mayer**

A mechanically controllable break junction (MCBJ) represents a fundamental technique for the investigation of molecular electronic junctions, especially for the study of the electronic properties of single molecules. With unique advantages, the MCBJ technique has provided substantial insight into charge transport processes in molecules. In this review, the techniques for sample fabrication, operation and the various applications of MCBJs are introduced and the history, challenges and future of MCBJs are discussed.

1. Introduction

In light of the rapid development of semiconductor technologies, the feature size of electronic devices is gradually approaching the miniaturization limits of silicon technology. At the same time, molecules are attracting more attention due to their remarkable properties. For instance, nanometer-sized molecules can be synthesized in large quantities at low cost, they are thermodynamically stable even at ambient conditions, and they possess structural variety and self-assembly, recognition, and quantum mechanical properties.[1–4] As early as 1974, Aviram and Ratner had predicted that individual molecules would someday be used as circuit elements in devices.[5] Today, a single molecule may represent the ultimate limit of what can be achieved so far. The dream of utilizing molecules as functional units in electronic circuits has motivated many researchers for years.[6] Compared to traditional electronic devices, molecular devices have many unparalleled advantages. First, the numerous degrees of freedom inherent in molecular structures may present previously unavailable functions. The promise of lower costs compared to semiconductors is attractive in manufacturing. Finally, the extremely reduced size of molecules may enable heightened capacities and faster performance and furthermore, provides the ability to surpass the limits of conventional silicon integrated circuits. Recently,

fundamental research of individual molecule-based devices such as molecular switches, molecular diodes, molecular transistors, and molecular charge storage have been reported.[2,7–9] More sophisticated molecular electronic circuits that can remember and process information are anticipated. Several recent reviews in the active field of molecular electronics are available.[2,6,10–12]

The prerequisite for a molecule-based device is to measure and control the charge transport through the molecule. For this purpose, molecular junctions are fabricated which can be distinguished as "many-molecule junctions" and "individual molecule junctions". In a many-molecule junction, normally a molecular monolayer is sandwiched between two electrodes,[13] which includes but is not limited to cross junctions[14] (cross wire or cross bar), liquid metal drop electrodes,[15] EGaIn contact junctions,[16,17] and nanopores.[18,19] In contrast, there are only few molecules, or single molecules trapped in the individual molecule junction, which include mechanically controllable break junctions,[7,20–22] scanning probe microscopy (scanning tunneling microscopy or conducting atomic force microscopy),[23,24] electrochemical deposition of nanogap electrodes,[25,26] and the electromigration breakdown method.[27–30] Among these methods, the mechanically controllable break junction (MCBJ) technique offers a continuously tunable gap size between two tip-shaped electrodes with impressive mechanical stability for the characterization of single molecules.[7,20–22]

MCBJ has proved to be a suitable and beneficial technique for molecular electronics due to its unique advantages. Many significant results, for instance, atom chain formation, single molecule conductance determination, and electron spin state control, have been achieved.[31–37] The MCBJ technique can be easily combined with other techniques, such as Raman spectroscopy, inelastic electron tunneling spectroscopy, and noise spectroscopy, to obtain fingerprint information of the molecules. However, there are still a number of challenges to overcome. From the fabrication point of view, the chips use polyimides as an isolating layer, which always suffer from a varied gap size due to its variable deformation at different temperatures. Regarding applications, MCBJs are inapplicable to measure the force and surface morphology, which can limit its utility. This review article focuses on the progress, extensive applications, and challenges of the MCBJ technique. Several new ideas and research topics related to the MCBJ technique have been proposed, which will aid in handling the challenges and promote further development of molecular electronics with MCBJs.

Dr. D. Xiang, H. Jeong, Prof. T. Lee
Department of Physics and Astronomy
Seoul National University
Gwanak-ro, Gwanak-gu, Seoul 151-747, Korea
E-mail: tlee@snu.ac.kr
Dr. D. Mayer
Peter-Grünberg-Institute
PGI-8, Bioelectronic
Research Center Jülich GmbH
and JARA, Fundamentals of Future Information Technology
Jülich 52425, Germany
E-mail: dirk.mayer@fz-juelich.de

REVIEW

The review consists of five sections. In the introductory section, we briefly present the motivations and goals that drive the field of molecular electronics. The second section describes experimental test beds for the measurement of electron transport through molecular junctions that possess individual molecules contacted to two solid electrodes. In the third section, we focus on the fabrication and utilization of the MCBJ technique for molecular electronics, which includes: 1) the chip fabrication progress; 2) the measurement of single molecule conductance, a basic property of the molecule; 3) the investigation of the complicated electrical behavior of molecules such as switches or diodes, which can lead to functional molecular devices; and 4) the electronic transport mechanism and control of the charge transport through molecules. In section four, we further discuss the combination of MCBJs with other techniques to extend their potential applications. Finally, we provide a summary and outlook in section five.

2. Test Beds for Molecular Electronics

2.1. Many-Molecule Junctions

The ability to electrically contact molecules with the external electrodes and control the electrical current through the molecular junctions presents an opportunity to understand the charge transfer in the junctions and explore the intrinsic physical properties of the molecules. Several solid-state device concepts have been developed in order to achieve this goal. The experimental test beds for molecular electronics can be grouped into two types: many-molecule junctions, presented in **Figure 1** (a-c), and individual molecular junctions, presented in Figure 1(d-f).[12] The number of trapped molecules, electrode geometry, electrical field, and interaction between molecules are different in these two types of molecular junctions. Each technique is unique in terms of contact formation, and each has advantages and disadvantages. A detailed introduction of testbeds for molecular electronics can be found in a previous review paper.[6,10] The basic idea of the many-molecule junction approach is to sandwich a molecular film between two electrodes. First, the molecules are immobilized on one electrode surface via a self-assembly process or Langmuir-Blodgett method.[38] A second electrode is then placed on top of the molecular film to form the junction. The placement of the top electrode is often the most difficult part in the fabrication process.

2.1.1. Micro-Scale Via-Hole Junction

Different strategies have been developed to form a molecular junction via-hole. A typical approach is using a nanopore.[35,39–41] A similar approach, in which a via-hole instead of a pore was fabricated on silicon substrate, was developed by Song et al.[42,43] With the nanopore and via-hole approach, a defined size of the contact area can be obtained, and these methods have been successfully employed to determine the intrinsic electronic transport properties of self-assembled monolayers (SAMs) of molecules. Unfortunately, filaments and electrical

Dr. Dong Xiang is a post doctor in the Department of Physics and Astronomy, Seoul National University, Korea. He graduated from China University of Geoscience and received his M.S. degree in 2006 from Huazhong University of Science & Technology, China. He received his Ph. D degree from RWTH Aachen University, Germany in 2011. His current research interests are single molecule study and optoelectronic devices.

Dr. Dirk Mayer received his Ph. D degree in Chemistry from University of Leipzig, Germany in 1999. After his post-doc at the Institute of Interface Science and Vacuum Physics, Forschungszentrum Jülich, with focus on charge transfer in organics adsorbates (1999–2002) he joined the Peter Grünberg Institute, Forschungszentrum Jülich as group leader. His main research areas are nanopatterning of bio-inorganic nanoconjugates and the investigation of charge transport processes in biomolecules.

Dr. Takhee Lee is an Associate Professor in the Department of Physics and Astronomy, Seoul National University, Korea. He graduated from Seoul National University, Korea, and received his Ph.D. from Purdue University, USA, in 2000. He was a post-doctoral researcher at Yale University, USA, until 2004. His current research interests are molecular electronics, polymer memory devices, nanowire electronics, and graphene-electrode optoelectronic devices.

shorts in SAMs are often formed upon vapor deposition of the top electrode, which limits the diameter of the nanopore junction to a few tens of nanometers.[43–45]

Akkerman et al. demonstrated another novel method for manufacturing molecular junctions with diameters up to 100 μm by spin coating a conducting polymer layer (PEDOT: PSS)
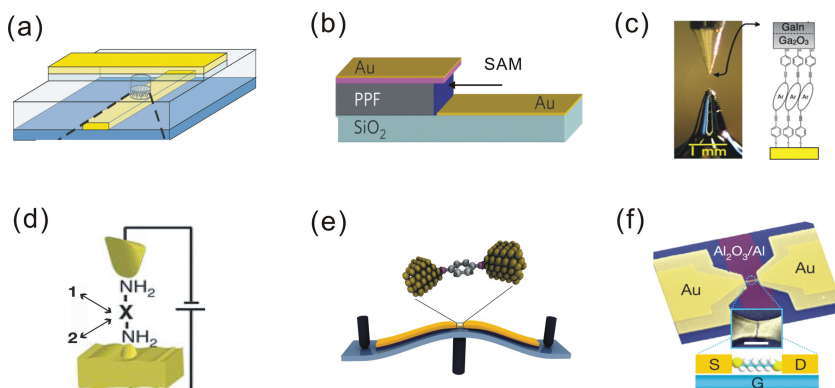
Figure 1. Test beds for molecule electronics. (a-c) Monolayer based junctions. (a) Conducting interlayer-based junction. Reproduced with permission.[44] Copyright 2006, Nature Publishing Group. (b) Surface diffusion mediated deposition. Reproduced with permission.[49] Copyright 2010, Nature Publishing Group. (c) EGaIn contact junction. Reproduced with permission.[1] Copyright 2008, American Chemical Society. (d-f) Individual molecule junction. (d) STM junctions. Reproduced with permission.[69] Copyright 2006, Nature Publishing Group. (e) Mechanically controllable break junction. (f) Electron immigration integrated with bottom gate. Reproduced with permission.[63] Copyright 2009, Nature Publishing Group.

between the SAM and top electrode, as shown in Figure 1a.[44] This PEDOT: PSS interlayer-based molecular junction exhibited a high device yield and efficiently avoided electrical shorts. The stability investigations reveal a shelf life of more than several months and no deterioration upon cycling.[46] Although the electrical properties of these molecular junctions may be influenced by the thermal treatment and morphology of the interlayer conducting film,[47] this simple approach can be potentially low-cost, compatible with the standard integrated circuit fabrication processes, and could pave the way for practical molecular electronics.[44,48]

2.1.2. Surface Diffusion Mediated Deposition

As previously mentioned, the vapor deposition technique frequently used to make the metal-molecule contact results in metal atoms penetrating or damaging the molecular layer. Bonifas et al. reported a new method of forming 'soft' metallic contacts on molecular layers through surface-diffusion-mediated deposition (SDMD), in which the metal atoms were deposited remotely and then diffused onto the molecular layer, thus eliminating the problems of penetration and damage. The SDMD approach, as shown in Figure 1b, includes several fabrication processes.[49] First, pyrolyzed photoresist films (PPF) were fabricated on silicon substrates. Then, a patterned etch mask (SiO$_2$) was fabricated on top of the PPF surface using optical lithography. A reactive ion-etching process was used to etch the unmasked PPF to create a near vertical sidewall with uniform undercutting beneath the etch mask. Subsequently, a molecular monolayer was attached to the PPF side wall by means of an electrochemical method in solution. Finally, metal contacts were deposited by electron beam evaporation in the direction perpendicular to the patterned mask. The electrical connection between the metal and the molecules was completed by surface diffusion of the deposited metal atoms towards the molecular layer. For SDMD, the influx of adatoms is controlled through

surface diffusion, ensuring continuous metal–metal binding as a perfect metallic contact. Soft contact molecular junctions fabricated by such method exhibit excellent yields. Moreover, in situ monitoring of the SDMD process can allow control of the progression from single/several molecules to many molecules.[50] The SDMD technique should be applicable to a more wide range in the future.

2.1.3. Liquid Metal Contact Junctions

Within a liquid metal contact experiment, a droplet of liquid metal is used either as the top contact, or both electrodes are provided by liquid metal drops. In the classical mercury drop experiment, two droplets of mercury are covered with SAMs and mechanically brought close together until a metal/molecule/metal tunneling junction is formed and the current across the molecule layer can be measured.[51] If just a single mercury droplet is utilized, a second planar electrode may be used, which should ideally be atomically flat (template stripped silver) and generate an Ag/molecules/Hg junction.[52] Nijhuis et al. also showed that combined with photolithography, small arrays of tunneling junctions based on liquid metal electrodes can be fabricated.[53] The liquid metal contact is quite stable and prevents problems encountered with evaporating metal top-contacts, such as avoiding metal atoms penetrating into the junction. Recently, a tip-shaped electrode reformed from an EGaIn droplet used to reduce the contact area was reported,[1,16,54] as shown in Figure 1c. The low toxicity, process ability, low-melting-point, and low reactivity of EGaIn in air render it a suitable candidate for electrode materials.[16] Please note the usual formation of a thin oxide layer when exposing liquid metals to air. Cademartiri et al. demonstrated that the charge transport through the molecular junctions was dominated by the SAM and not by the oxide layer or by the contaminants.[54]

2.2. Individual Molecular Break Junctions

Monolayer junctions are excellent approaches to obtain statistical information of molecules. However, sometimes it is important to know the properties of individual molecules, especially single molecules in which the inter-molecular interaction can be excluded, which will lead to single molecule electronic devices. Currently, with the rapid development of micro-fabrication, many techniques can address individual molecules, even single molecules.[3] These techniques include but are not limited to the following: surface-mediated metal deposition with a shield,[50] covalently bridging gaps in single-walled carbon nanotubes,[55] electromigration technique, scanning probe technique, and mechanically controllable break junction techniques. Within the scope of this review we only present a part of examples.

2.2.1. Electromigration Based Break Junctions

Electromigration had once been considered a failure mode in microelectronic circuitry. However, it has recently been well utilized to fabricate nanogap electrodes for molecular junctions.[28,29,56–58] The passage of a large density current to a thin metal wire predefined by lithography causes the electromigration of metal atoms and eventual breakage of the nanowire. This process can yield a stable electrode separation as small as a few nanometers. Much progress has been made with electromigration techniques during the last decade. Strachan et al. prepared nanogaps by the electromigration approach with transparent SiN$_x$ membranes to permit the use of transmission electron microscopy to image the gap in situ.[59] With this method, the break process and corresponding geometry could be observed in real time. Johnson et al. developed a feedback controlled electromigration technique for the parallel formation of nanogap electrodes, which was promising for constructing large scale circuits of molecular devices.[60] The electromigration approach can also be applied to carbon nanotubes to fabricate a nanogap for molecular electronics.[61,62] Furthermore, electromigration is a very nice method to prepare three-terminal nanodevices with the gate effect (Figure 1f).[63–65] One major issue that needs to be addressed when dealing with the electromigration process is Joule heating. Although Joule heating is partially needed to start the nanogap formation process, excessive heating can cause unexpected melting of the metal. The possible formation of metal debris and metal islands due to metal melting would interfere with the insertion of target molecules and most likely screen the desired signals.[66,67]

2.2.2. Scanning Probe Techniques

Single-molecule study was first enabled by the development of scanning probe microscopies in the 1980's, which include scanning tunneling microscopy (STM) and conducting probe atomic force microscopy (CP-AFM). The strength of STM lies in its combination of high-resolution imaging and spatially scanning tunneling spectroscopy.[68] In the STM break junction, a metal/molecules/metal junction is quickly and repeatedly formed between the substrate and the tips by moving the STM tip into and out of contact with a metal electrode surface containing adsorbed molecules, as shown in Figure 1d.[69] With STM techniques, many significant results concerning molecular properties have been obtained.[69–72] Furthermore, in situ STM allows a shift in the position of the molecular states with respect to the Fermi level of the electrodes via an electrochemical gate.[73,74] In CP-AFM, the metal-coated tip, acting as the top electrode, is gently brought into contact with molecules assembled on the bottom electrode and electron transport properties while the applied force can be measured simultaneously.[23,75,76] Therefore, it is a powerful tool to investigate the relationship between conformation and charge transport in a molecular junction. Please note, CP-AFM is a SAM-based technique definitely, but a single molecule can also be addressed when pulling the point contacts apart.[23] The main obstacle is that the CP-AFM tip, coated with a metallic layer, is larger than an atomically sharp STM tip so spatial resolution is lower than STM. Moreover, the top contact between the tip and the molecule

is often less well defined due to its large size. Some novel ideas have been put forth to reduce this problem, for example, embedding a molecule of interest into the matrix of another type of less conducting molecules,[71,77] or binding nanoparticles between the molecules and the CP-AFM tip.[78]

One of the challenges in molecular electronics is to fabricate electrodes separated with a nanogap that can fit a sample molecule precisely and measure the properties of various types of molecules. This difficulty has been overcome by bringing two electrodes mechanically together or separating them by means of a MCBJ. With MCBJs, the gap size between the two electrodes can be precisely and continuously adjusted. MCBJ techniques are described in further detail in the following sections.

3. Mechanically Controllable Break Junctions

3.1. Principle and Advantages

A schematic of a common state-of-the-art break junction setup is shown in Figure 1e. A small piece of a metallic wire is fixed on a flexible substrate, called a bending beam. In general, the cross section of the wire is reduced between two fixed points by making a notch near the middle of the wire. The bending substrate is normally fixed at both ends by counter supports. A vertical movement of the push rod, which can be precisely controlled by a piezoelectric actuator or motor, can exert a force on the bending beam. As the beam is bent, the metal wire starts to elongate, which results in the reduction of the cross section at the notch and finally results in a complete fracture of the metal wire. After breaking the metal wire, two clean facing nanoelectrodes are generated. The distance between the electrodes for both the opened and the closed directions is controlled by the bending or relaxing of the substrate, respectively. After integrating the molecules into the gap, they may bridge the two electrodes and the electronic properties of the molecules can be determined.

The MCBJ technique has many advantages; for example, the MCBJ setup can be easily integrated into other systems, such as a Raman spectrometer or high vacuum system, due to its open and flexible configuration. The influence of contaminants is reduced because a fresh break cross section of the gold bridge is created in the MCBJ experiment. With advanced lithography techniques, the electrode can be scaled down to molecular dimensions, which is very suitable for single molecule measurements. The unique advantage of the MCBJ technique is the high mechanical stability of the system. The electrodes are rigidly fixed to the substrate at a short distance (approximately 0.5 mm by traditional fabrication, and approximately 1 μm by lithography fabrication), so the length of the free standing parts is much shorter than in a typical STM setup, resulting in a very high resonance frequency. Furthermore, due to the mechanical configuration of the three point bend apparatus, the vertical motion of the push rod (ΔX) causes only a highly reduced horizontal displacement (ΔZ) of the electrodes (Δz/Δx >10000). This means that any disturbing effect from the push rod (for instance vibration, thermal expansion or voltage instability upon the piezoelectric component) can be strongly reduced on the junction. The movement of the push rod can be

Materials
Views
www.MaterialsViews.com

ADVANCED
MATERIALS
www.advmat.de

REVIEW

controlled with sub-micrometer accuracy, which means control of the gap with sub-angstrom precision and precise control of the mechanical stress, rendering this technique highly suitable for single molecule measurement.

In addition to the important advantages of the MCBJ technique, the main disadvantages are the uncontrollable details of the breaking process. For instance, the local shape of the electrodes and the atomic configurations of the electrodes are unknown. MCBJs cannot be scaled in a manner similar to crossbars to address a specific cross-section, which limits the potential applications in information processing. Also MCBJs cannot obtain the surface topography of the sample like scanning tunneling microscopy. Nevertheless, as a fundamental research technique, MCBJs are powerful, especially for investigations of single molecule properties.

3.2. Progress in MCBJ Chips Fabrication

The idea of the MCBJ was put forward by Moreland and Ekin to investigate tunneling characteristics for superconductors in 1985[79] and further developed by Muller and van Ruitenbeek for the investigation of atomic point contact in 1989–1992.[80,81] This method was then adopted creatively by Reed and co-workers to measure the properties of single molecules in 1997.[35,39] The first MCBJ chip used by Moreland et al. was fabricated twenty years ago by gluing a Nb-Sn filament on a flexible glass beam.[79] Since then, chip fabrication has made significant progress. The approach to define electrodes has gone through three stages: mechanical cutting, electrochemical deposition and micro-fabrication by electron beam lithography. Currently, not only two-terminal chips are fabricated, in which the electron transport through molecules can be measured, but also three-terminal chips can be obtained, in which the electron transport properties can be controlled.

3.2.1. Two-Terminal Chips

An early stage chip for a MCBJ is shown in **Figure 2**a. A metal wire, typically hundreds of micrometers in diameter, was fixed onto a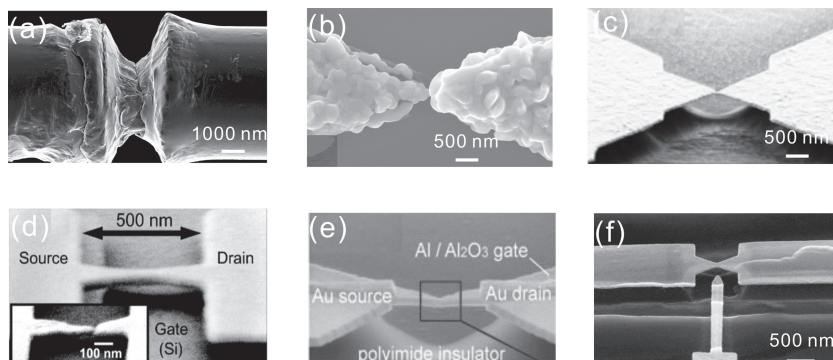n insulated elastic substrate with two drops of glue very close to either side of the notch.[79] The notch was manually cut into the center of the metal wire by knife. Another method to make a notch in the middle of the metal wire was chemical etching.[82] For instance, tungsten wire can be electrochemically etched by immersing it in an etchant solution at the middle of a platinum loop, which was set on the surface of a KOH solution. When an AC voltage was applied between the tungsten wire and the platinum loop, part of the tungsten near the solution surface was etched, and a corresponding notch was fabricated.[83] The disadvantages of the macro-wire based fabricated chips are the following: (1) the large size of the electrodes with rough surfaces reduces the reproducibility of the breaking process, (2) contamination during the fabrication process may occur, and (3) there is a limited attenuation factor, and the corresponding mechanical stability is unimpressive.

The chips for the MCBJ experiment can also be fabricated by electrodeposition on template electrodes that were predefined on the substrate by optical lithography.[21,26,84–86] The initial electrodes, with a relatively large gap, are fabricated by lithography techniques on substrates, e.g., SiO$_2$. The gap is then narrowed, even fused, by depositing specific atoms onto the electrodes. The inter-electrode distance can be decreased or increased on the atomic scale through the depositing mode and dissolution mode, respectively.[87] For instance, we reported an approach for the fabrication of facing nanoelectrodes by gold electrodeposition, where the morphology of the electrode surface was modified by the applied electrochemical potential. This created nanoelectrodes with rounded surfaces at high overpotentials and needle-like surfaces at low overpotentials, as shown in Figure 2b.[85,88] Recently, electron beam lithography and reactive ion etching techniques were utilized for chip fabrication on a flexible substrate.[34,89–98] Figure 2c shows a typical micro-fabricated chip for a MCBJ.[99] The chip fabrication process consists of several steps: (1) an isolating layer (polyimide, several μm thick) is spun onto the substrate; (2) standard e-beam lithography process is performed to define the metal wire; and in the final step, (3) the isolating layer is isotropically dry etched to obtain a suspended metal bridge. Several groups have reported such micro-fabricated chips with various electrode layouts that are suitable for individual molecule measurements with excellent mechanical stability.[36,91,94,96,98,100,101]

3.2.2. Three Terminal Junctions

With two terminals, one can only sweep the Fermi level of one electrode with respect to the second electrode and the molecular states. With three electrodes, one can shift the molecular states with respect to the Fermi levels of both electrodes. This extends the functionality of the break junction significantly to controlled electron transport through the molecule. Champagne et al. demonstrated a device geometry for single-molecule electronic experiments that combined both the ability to adjust the spacing between the electrodes mechanically and the ability to shift the energy levels in the molecule using a bottom gate electrode, as

Figure 2. Typical kind of chips for MCBJ. (a) mechanical cutting on gold wire. (b) Chemical deposition. Reproduced with permission.[85] (c) E-beam lithography on flexible metal substrate. Reproduced with permission.[99] (d) Bottom gating with a doped silicon substrate. Reproduced with permission.[103] Copyright 2005, American Chemical Society. (e) Back gate directly contacted with the source and drain electrode. Reproduced with permission.[66] Copyright 2010, Institute of Physics. (f) Side gating with a nano metal electrode.

shown in Figure 2d.[36,102,103] To fabricate the devices, a thick SiO_2 film was first grown on top of a degenerately doped silicon wafer. A lithography liftoff process was performed to pattern the gold wire, which was connected to larger area contact pads. Then, hydrofluoric acid was used to remove the SiO_2 under the Au bridge, suspending it above the silicon substrate, which worked as the gate electrode. In such a device, the amount of bending allowed by the brittle Si chip is generally not sufficient to break the metal bridge solely through mechanical motion. Therefore, an initial break of the wires, partially or fully using electromigration, to make nanoscale gaps for molecule measurement is needed.[29,30,57]

Martin et al. introduced a new device architecture for the independent mechanical and electrostatic tuning of nanoscale charge transport, as shown in Figure 2e.[66] In contrast to previous gated mechanical break junctions that have a gap between the source-drain electrodes and the gate electrode,[36,102,103] the source-drain electrodes were directly deposited on the gate dielectric, and the source-drain together with the gate electrode were suspended above the substrate. Throughout the bending-controlled tuning of the source-drain distance, they demonstrated that the electrical continuity of the gate electrode was maintained. The mechanical and electrical control of charge transport through the nanoscale island was successfully demonstrated. However, to break the thin gold bridge in such a geometry, much larger substrate bending was required. The available gap size range was limited to a few angstroms due to the extremely small attenuation factor, which may be improved with an additional electromigration process.[66]

Compared with the bottom gating that was introduced above, we proposed a new design of MCBJ chips by adding a side-gate electrode near the source-drain electrode. By means of electron beam lithography and reactive ion etching, a suspended metal bridge was fabricated. Simultaneously, a nanoscale metal gate electrode was fabricated on the shoulder, which is located a few nanometers away from the suspended metal bridge, as shown in Figure 2f. With this configuration, the gate electrode remains unchanged (the fracture of the gate electrode can be completely avoided) when one tries to break the metal wire and to obtain a large gap size by deeply bending the substrate.

3.3. Single Molecule Conductance Measurement

The first molecule that was electrically characterized by MCBJ experiments was 1,4-benzenedithiol by Reed et al.[35] In their experiment, a notched metal wire glued onto a flexible substrate was fractured by bending the substrate, as shown in **Figure 3**a. After breaking the metal wire, the molecules of benzene-1,4-dithiol self-assembled onto the two facing gold electrodes to form statically stable gold-sulfur-aryl-sulfur-gold
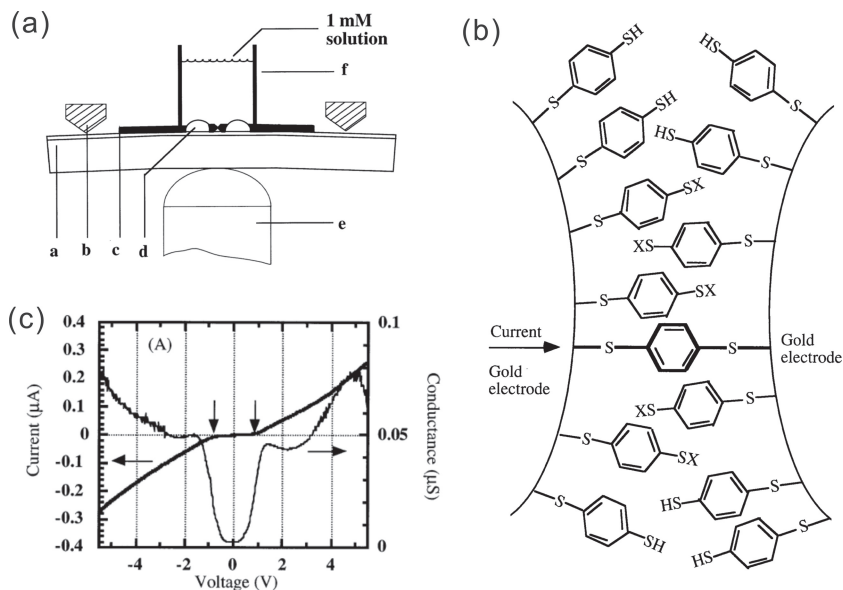

Figure 3. The measurement of single molecule properties with MCBJ. (a) A schematic of the MCBJ junction. (b) A schematic of a benzene-1,4-dithiolate SAM between proximal gold electrodes formed in an MCBJ. (c) Typical $I(V)$ characteristics, which illustrate a gap of 0.7 V; and the first derivative $G(V)$, which shows a step like structure. Reproduced with permission.[35] Copyright 1997, AAAS.

junctions by bringing the two electrodes close to each other, enabling direct observation of charge transport through the molecules, as shown in Figure 3b. Two steps of the conductance-voltage curves, with a highly reproducible apparent gap at approximately 0.7 V, are shown in Figure 3c. The reproducibility of the minimum conductance at a consistent value implies that the number of active molecules could be as few as one. This study provides a qualitative measurement of the conductance of a junction containing an individual molecule, which is a fundamental step forward in the emerging area of molecular-scale electronics. After this experiment, a number of model molecules, such as hydrogen, were investigated.[34] Presently, the electrical properties of a single molecule can be measured in different environments.[93,104] Moreover, the conductance of sophisticated molecules, for example metal complex molecules and biomolecules, has been investigated by this method.[89,105,106]

3.3.1. Directly Determining Single Molecule Conductance

Although metal–molecule–metal links have been investigated by STM techniques, it is difficult to unambiguously establish that a single molecule forms the contact. Smit et al. distinctly showed that a single hydrogen molecule can form a stable bridge between platinum electrodes, and the conductance of a single hydrogen molecule can be directly determined by a statistical method.[34] To extract the common features of these conductance curves, a large series of conductance curves was collected and converted into a conductance histogram. The main panel in **Figure 4** shows a histogram for Pt contacts (black) without a molecule, in which a dominant peak at 1.4–1.8 G_0 was observed. A new clear peak at approximately 1 G_0
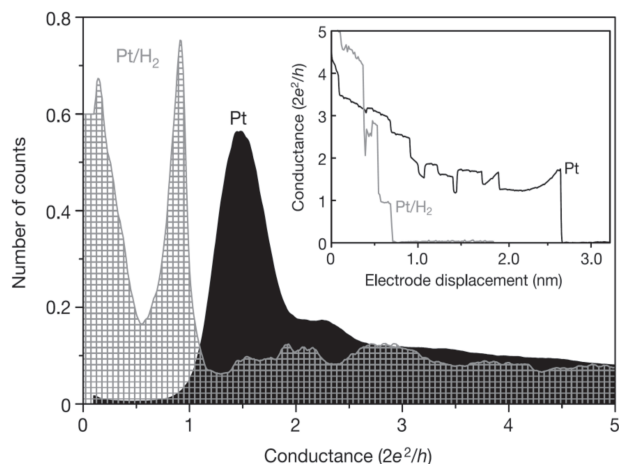
Figure 4. Conductance curves and histograms for clean Pt, and for Pt in a H$_2$ atmosphere. Inset, a conductance curve for clean Pt (black line) and Pt/H$_2$ (gray line) during break process at 4.2 K. Reproduced with permission.[34] Copyright 2002, Nature Publishing Group.

was observed when the hydrogen was introduced. This new typical conductance peak was attributed to the single hydrogen-bridged Pt-H$_2$-Pt molecule junction. In contrast to results with organic molecules, the bridge had a nearly perfect conductance of one quantum unit carried by a single channel. This experiment represents a nice test system for the investigation of fundamental transport properties of single-molecule devices.

3.3.2. Robust Statistical Analysis

In some cases, there are poor agreements in the reported conductance values of single molecules, e.g., due to different contact configurations. To overcome junction–to–junction fluctuations, statistical analysis has been utilized through conductance histograms.[107] Peaks in the histogram indicate preferred and stable junction configurations. The observation of a series of conductance values appearing at multiples of a fundamental value can be considered evidence for the formation of few-molecule junctions. However, data selection schemes have been partially applied to build effective histograms. Gonzàlez et al. proposed a new method to build a histogram in log G rather than G.[96,108] They chose octanedithiol junctions as the target molecule, and the conductivities were measured through a mechanically controllable break junction. The conductance histograms, which were generated in log G, always showed the typical peaks with and without data selection. This observation means the conductance value assigned to a single molecule was robust and that the data selection did not improve the histogram built in this manner. Most of the conductance histograms were built using current–distance stretching curves. Hong et al. demonstrated that conductance histograms can be obtained using $I–V$ curves, and the results agree well with other approaches.[109] Reuter et al. presented a detailed analysis of peak features of conductance histograms and found that histograms possessed high information content and were not limited to a simple conductance value.[110] They demonstrated that resonant and nonresonant tunneling present different features in the conductance histogram, and additional interpretations

can be extracted from experimental statistical data. Nevertheless, conductance histograms normally cannot be used to distinguish between structurally different configurations with similar conductance values or to obtain information concerning the relationship between conductance and junction elongation.[111] Makk et al. proposed a novel statistical analysis method based on the two-dimensional cross-correlation histogram (2DCH). They demonstrated that this method provides new information about the relation of different junction configurations that occur during the formation and evolution of metal and single-molecule junctions.[111,112]

3.3.3. Conductance Measurement in Liquid

Compared with the experiment performed in a vacuum, the electrical measurement in solution is more challenging due to the solvent effect. Solvent turbulence-induced noise, capacitive charging, and molecule polymerization should be considered in liquid environment. Moreover, the intrinsic transport mechanisms may be influenced by solvent molecules.[113] Grüter et al. present a break junction setup with an integrated liquid cell, which allows exploration of the influence of solvents on the electronic properties of atomic contacts.[113] The variation of the electrical conductance with different types of solvent during the electrode separation process was investigated. They observed a systematic and reproducible trend in the variation of the tunneling barrier height with different solvents. After further research, Grüter et al. presented electronic transport measurements through one end thiolated C$_{60}$ molecules in a liquid environment by means of MCBJ.[114] When the electrode separation of the molecule-modified junction was varied, they observed a peak in the conductance traces. Moreover, the shape of the conductance curves was strongly influenced by the solvents. With a resonant tunneling model, they extracted the electronic tunneling rates that governed the transport properties of the junction. Huber et al. determined and compared the electrical conductance of four conjugated molecules at the single molecule level and under identical liquid environmental conditions, as shown in **Figure 5**.[96] Their results showed that the conductance of oligo (phenylene vinylene) (shorthand OPV, top row) was slightly higher than that of oligo (phenylene ethynylene) (shorthand OPE, second row). They also found that it was difficult to distinguish between the OPV and two modified OPVs with side groups. In other words, the solubilizing side groups do not noticeably influence the conductance values of such conjugated molecules. A main advantage of the experiment in liquid is the use of an electrochemical gate. Adding a chemically controllable environment in break junction experiments would offer many interesting possibilities, for instance, adjusting the redox state using a liquid gate.[74,115]

3.3.4. Metal Complex Molecules

Metal ions play a crucial role, for instance, in biological charge transport, and a metal complex molecule can also potentially be used for electronic devices.[116] It is of fundamental interest to investigate if, and how, metal ions influence electron transport on the level of individual molecules.[117] However, little is known
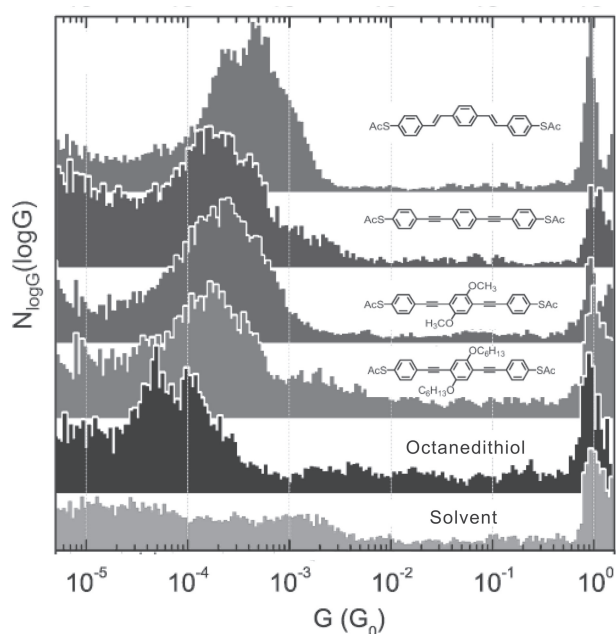
ADVANCED
MATERIALS
www.advmat.de

Materials
Views
www.MaterialsViews.com

REVIEW

Figure 5. Measurement of single molecule conductance with MCBJ in solution. Log-histograms of measured conductance values log (G(z)) obtained during one hundred successive open cycles. From top to bottom, the histograms show data for OPV (first row), OPE compounds (from second row to four row), and the two references, octanedithiols in mesitylene and the solvent alone. It is shown the conductance of OPV is higher than that of OPE. The OPE with varied side groups shows similar conductance. Reproduced with permission.[96] Copyright 2008, American Chemical Society.

about electron transport via metal ions trapped between ligand molecules. The binding of a metal ion to a single host molecule (peptide) was investigated at the single molecule level by Xiao et al., and they found conductance of the peptide upon the metal-peptide bonding significantly increased.[105] The charge transport depends on the nature of the ligands but also on the type of metal ion entrapped in the complex. We investigated the influence of different metal ion species in a system where the ligands remain essentially unchanged.[106] In the experiment, 3,3′-dithiobis[N-(5-amino-5-carboxypentyl) propionamide-N′,N′-diaceticacid]dihydrochloride (C$_2$-NTA) was used as the host molecule. The corresponding conductance histogram in **Figure 6**a showed two series peaks. Breaking a metal junction modified by (C$_2$-NTA) generated a clear peak near $P^1_0 \approx P_0^2 \approx P^3_0 \approx 1.1 \times 10^{-4}$ G_0. However, after an additional metal ion was introduced, a new set of peaks (P_A, P_B, P_C) in the conductance histogram was observed (Figure 6b–d), which dependeds on the type of introduced metal ion. In this way, we demonstrated that the surface tethered nitrilotriacetic acid molecules formed stable

metal-molecule-ion-molecule-metal junctions with different metal ions, and the conductance of the junctions depended strongly on the type of metal ion that was integrated, in the following order: Ca^{2+} > Zn^{2+} > Ni^{2+}.

3.3.5. Orbital Determined Molecule Conductance

Although several important factors affect electron transport, such as molecular length, molecular conformation, and applied bias voltage, the molecular orbital (MO) amplitude near the Fermi energy has shown reliable guidelines for understanding molecular conductance.[22] Orbital amplitude analysis, based on first principle calculations, revealed that delocalization of the orbital is critical for a good conduction pathway.[118] Yoshizawa et al. developed a chemical method by understanding of electron transport in molecules in terms of the frontier orbital theory. They predicted that the phase and amplitude of the highest occupied molecular orbital (HOMO) and lowest unoccupied molecular orbital (LUMO) of π-conjugated molecules determine the properties of electron transport.[119] Recently, they confirmed these theoretical predictions experimentally by using mechanically controllable break junctions to measure the conductance of single naphthalene dithiol derivatives.[22] Their measurements showed that the conductance of symmetry-allowed 1,4-naphthalene dithiol exceeds that of the symmetry-forbidden 2,7-naphthalene dithiol by 2 orders of magnitude. Because the HOMO and LUMO levels and the HOMO-LUMO gaps are similar in these derivatives, they attributed the difference in the measured molecular conductance to the difference in the phase relationship of the frontier orbitals. They noted that the phase, amplitude, and spatial distribution of the frontier orbitals provided a way to rationally control electron transport properties within molecules.
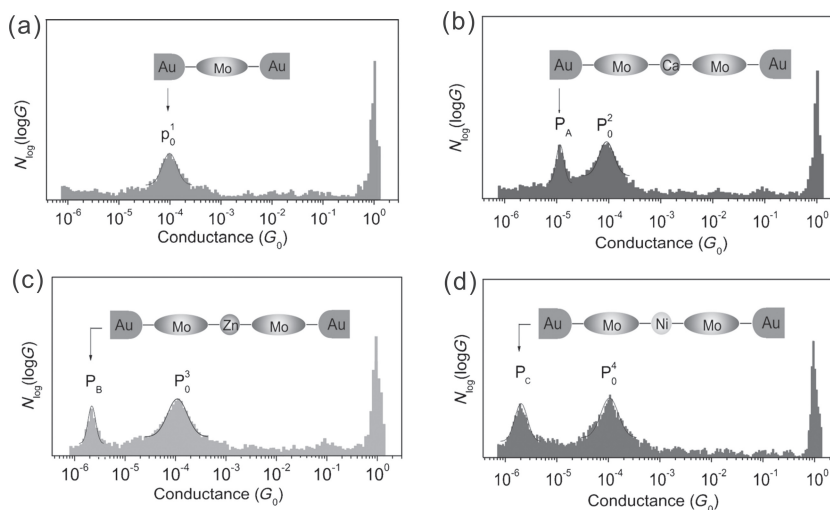

Figure 6. Conductance investigation of metal complexes at single molecule level. a) Log histograms of measured conductance when dithiobis (C$_2$-NTA) was applied to the junction. Only one peak can be clearly observed. (b–d) Conductance histogram of molecules junction bridged by Ca^{2+}, Zn^{2+}, Ni^{2+}, respectively. An additional peak is present. The peaks P^1_0, P_0^2, P^3_0, P_0^4 are located at the same position and can be assigned to the conductance of metal-molecule-metal junctions. While the position of P_A, P_B, P_C is dependent on the type of bridged metal ion. Reproduced with permission of The Royal Society of Chemistry.[106]

3.4. The Remarkable Properties of Molecules

Compared to silicon technology, molecular systems possess many advantages: they represent confined stable units, can self-assemble into more complex functional units, have a large structural variety, and perform defined conformational changes. With the MCBJ technique, several remarkable properties of molecular systems were studied, such as switching, negative differential resistance (NDR), diode and rectification, the Kondo Effect, and π–π orbital coupling. Each of these remarkable properties can lead to a molecular device with a special function. Here, we present a few examples.

3.4.1. Switching

The stochastic switching phenomenon that appears in the molecule junction is often attributed to fluctuations in the molecule–metal contact.[120] However, if the switch behavior is sensitive to a controllable stimulation, it can lead to potential electronic devices. In the past decade, detailed investigation has been performed on a great variety of molecular switches, including redox-active molecules, mechanically interlocked switches, and photochromic switches.[2,4] Lörtscher et al. demonstrated that a single molecule connected to two symmetric leads in a two-terminal configuration can be reversibly and controllably switched between two stable states in response to an external voltage stimulus.[99] In this geometry and under a very controlled environment using the MCBJ technique, they excluded the inter-molecule effect and contact effects. They proved that the observed switching truly had a molecular origin and attributed it to the effect of the nitro group in the molecule. Their results indicated that potential molecular switch devices can be fabricated with the appropriate molecular design.

Controlling current in a molecule with light stimulation may lead to optoelectronic switching devices.[121] One mechanism of photoswitching is through light-induced conformational changes in the molecule. Optical one-way switching of photochromic dithienylethene from the conducting to the insulating state has been demonstrated by Dulik et al. when illuminating the molecule with visible light.[122] Upon illumination, the molecule transitioned from close state to open state, and a corresponding increase of resistance was observed. However, the reverse process, which should occur upon a second illumination with the appropriate UV light, was not observed. The one-way switching properties were attributed to quenching of the photo-excited closing reaction because the HOMO level of the open isomer overlaps with the high density of states of the Au electrode, which facilitates fast electron transfer to the molecule and eventually shortens the lifetime of the hole. Following this study, the quenching problem was solved and reversible conductance switching in diarylethenes was observed
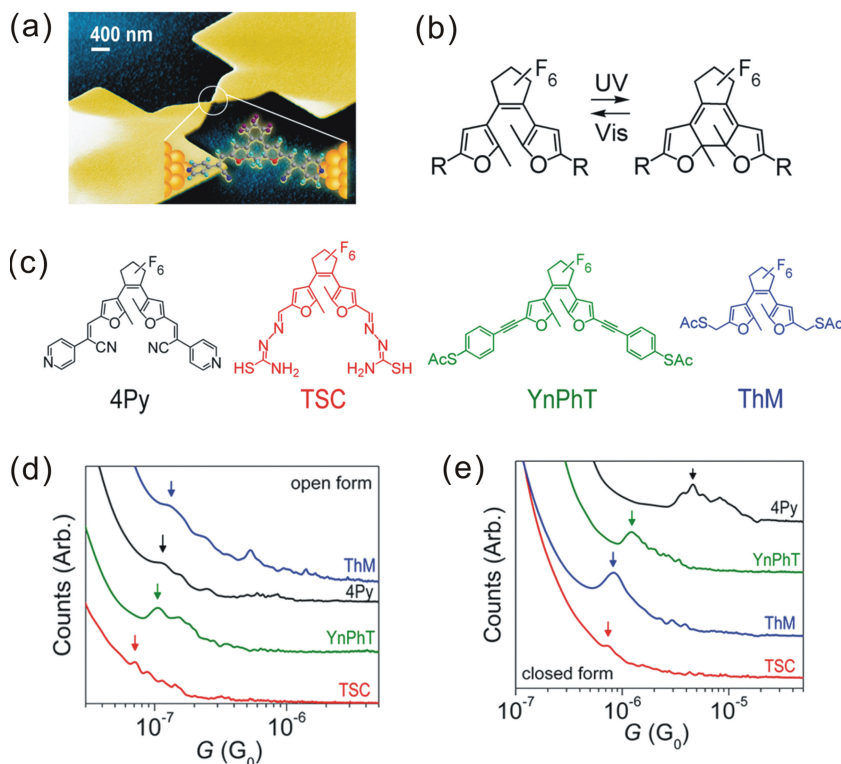

Figure 7. Photo induced witching. (a) Scanning electron micrograph of the MCBJ device and an illustration of an Au–4Py–Au junction. (b) Sketches of open (left) and closed (right) forms of photochromic molecules (difurylethenes). (c) Structures of the four different molecules, 4Py, TSC, YnPhT, and ThM, respectively, (d,e) Conductance histograms of photochromic molecular junctions for open and closed forms of all four molecules. Reproduced with permission.[91] Copyright 2012, American Chemical Society.

using a highly conductive organic top electrode.[123] Two-way photoswitching and the corresponding charge transport characteristics of a single molecule were systemically investigated by Kim et al.[91] Sulfur-free diarylethene molecules were developed and studied via electrical and optical measurements. The single-molecule conductance and the current-voltage characteristics were measured in a MCBJ system at low temperatures. They showed that the side chains and end groups of the molecules are both crucial to understand the charge transport mechanism of reversible photoswitching molecular junctions, as seen in **Figure 7**. It can be seen that all four types of molecules increased in conductance after transitioning from the open (Figure 7d) to the closed state (Figure 7e). The 4Py molecule possessed side chains consisting of pyridine end groups, which helped to establish a very direct link between the molecular π-system and the metallic surfaces. This structure led to a relatively large signal ratio of conductance, e.g., the high ratio between the single-molecule conductance in the closed form and that in the open form. The opposite phenomenon is light emission as a result of current passing through the molecular junction, which has not been investigated with MCBJs.[124] The main technical challenge is the detection of light emitted from a single molecule. The integration of light switchable molecules is an emerging approach, with many potential applications in addition to investigation of photochemical processes on the single molecular level.

3.4.2. Rectification and Diode

Molecular rectification consisting of an asymmetric current response of a molecular junction to an external voltage bias was first predicted by Ratner et al.[125] Normally, three mechanisms (the Aviram-Ratner model, Kornilovitch-Bratkovsky-Willians model, and Datta-Paulsson model) were used to explain rectification behavior, in addition to the case with asymmetric electrode-molecule coupling at both ends.[7] The Aviram-Ratner approach considers a donor–insulator–acceptor configuration, where two electrodes are connected through three tunneling barriers.[125] The underlying mechanism of the Aviram-Ratner approach uses the electric field to shift the energy levels of the molecular orbitals (HOMO or LUMO) according to their asymmetric energetic positions in the gap. Later, this mechanism was generalized by Kornilovitch, Bratkovsky, and Willians to a simpler system with only one molecular orbital, referred to as the KBW model, in which the electron tunneled through asymmetric tunneling barriers.[126] In this approach, the position of the orbital is not located symmetrically between the electrodes. The molecular orbital can be aligned or separated with the Fermi energy of the electrodes depending on the bias direction, which will result in the rectification behavior. Datta et al. considered a symmetrical shift in the conducting orbital with respect to the applied bias. However, unequal coupling and the consequent difference in charging effects led to different tunneling rates between the orbital and the two electrodes. In the resonant tunneling condition, the average population of the orbital strongly depends on the bias direction, leading to rectification behavior (Datta-Paulsson model).[127] The latter two mechanisms differently impact on the current-voltage characteristics: the asymmetric field mechanism leads to a shift in the onset voltage for resonant tunneling depending on the bias direction; the asymmetric charge leads to a different differential conductance in the region of resonant tunneling.[7] Both the influence and high rectification ratio were observed by Lörtscher et al. in their MCBJ experiment, as shown in **Figure 8**.[7] They proposed a simple two-level model consisting of a di-block molecule, as illustrated in inset of Figure 8. This "combined model" uses

semi-empirical formalism[128] to combine the mechanisms of level shifting due to field and charging effects. The voltage-current curves simulated by the "combined model" showed excellent agreement with the experimental data.

An extreme case of rectification is a diode, which facilitates current flow in one bias direction and suppresses current in the opposite direction. Single-molecule diodes, which show step-like features of I–V, have been fabricated using a lithographically defined MCBJ by Elbing et al.[129] The molecules consist of two weakly coupled electronic π-systems (donor-acceptor structure) with mutually shifted energy levels. The results indeed showed diode-like current-voltage characteristics, with a current ratio up to 10. Their corresponding theoretical analysis suggested that the bias dependence of the polarization of the molecule fed back into the current, leading to diode behavior.[129] In brief, two separated π-systems can be viewed as two quantum dots coupled in series, and the electronic orbitals are localized on one of the dots. When one sweeps the bias voltage, the electronic levels of both dots are shifted with respect to the another, and two levels will cross each other at certain voltages. Whenever an unoccupied level passes by an occupied one, an additional transport channel is opened for inelastic transmission from one dot (donor) to another dot (acceptor). With each additional transport channel, the current grows substantially, demonstrating the stepwise feature in the I–V curves.

3.4.3. NDR Behavior

A region of decreasing current with increasing voltage in the I–V curve is referred to as negative differential resistance (NDR). In the molecular aspect, Hg-alkanethiol/arenethiol-Au molecular junctions were used to develop a physical model for the hysteretic negative-differential resistance (NDR). It was concluded that the NDR was caused by slow charge capture (reduction or oxidation) during the forward sweep and the resultant effect on tunneling.[130] Reed and co-workers observed large ratio NDR behavior in OPE molecular junctions substituted with nitro and amino groups on the central ring.[18] They suggested that a possible mechanism for NDR was a two-step reduction process that modified charge transport through the molecule. With MCBJ techniques, the NDR behavior at the single molecule level was successfully observed.[101,131] Lörtscher et al. acquired non-linear current voltage (I–V) characteristics at variable temperatures.[101] DNR behavior was observed with electron resonant tunneling through the molecule junction, in which the voltages accessing the first molecular orbitals in resonance were applied. Their results provided spectroscopic information concerning the junction's energy landscape, in particular about the molecular level alignment with respect to the Fermi energy of the electrodes. Kang et al. showed that the current-voltage (I–V) characteristics of a molecule junction in an aqueous solution displayed a series of NDR and hysteresis behaviors.[126] Under high-vacuum conditions, the peak positions of the NDR can still be observed but are shifted to lower voltages with reduced amplitude. The observed NDR behavior in a DNA molecular junction was explained by a polaron model, which led to a shift of the molecular level upon charging.[131] Because gate electrodes can be integrated into MCBJ devices, it will be
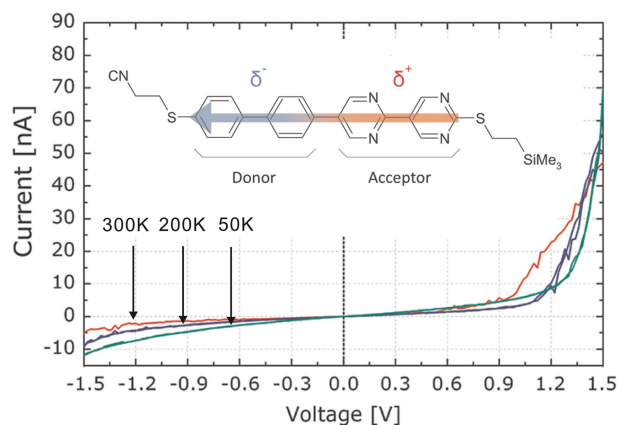
Figure 8. I/V traces for the Au-SB diode-Au junction recorded at temperatures ranging from 300 to 50 K. The inset shows the structure of the molecule. Reproduced with permission.[7] Copyright 2012, American Chemical Society.

interesting to experimentally demonstrate NDR behavior in a three terminal configuration with MCBJs in the future[115]

3.4.4. Kondo Resonance

An idealization of zero-bias Kondo resonance is the Anderson single level impurity model, where the magnetic impurity is viewed as having one energy level with an unpaired electron.[132] It is classically forbidden to bring the electron out of the impurity without adding energy into the system. However, the uncertainty principle does allow this to happen via an exchange process.[132] That means the electron is allowed to jump off the magnetic impurity and onto an electrode. During this time, another electron from the Fermi sea must jump onto the impurity to replace the remaining one. The coherent superposition of such co-tunneling events results in the screening of the local spin of the impurity, thereby producing the Kondo resonance, in which a new transport channel appears at zero bias and a conductance peak at zero bias will be observed.[133] However, the precise control over the spin degrees of freedom with most quantum dots in the study of Kondo phenomena is difficult. Molecules incorporating transition-metal atoms provide powerful new systems in this regard because the spin and orbital degrees of freedom can be controlled through well-defined chemistry.[134] Liang et al. reported the observation of Kondo resonance in single-molecule transistors, where an individual divanadium molecule served as a spin impurity.[64] They found that the Kondo resonance peak could be tuned reversibly by using the gate voltage to alter the charge and spin state of the molecule. Recently, a new phenomenon (underscreened Kondo effect) was observed by Parks et al. using the MCBJ technique.[36] This significant achievement will be further discussed in section 3.6.

3.4.5. Lateral π-Orbital-Coupling

A remarkable property of some molecules is lateral π-orbital-coupling, which exists between π-orbitals of the molecule and the orbitals of the attached electrodes.[135] This lateral coupling is well known to cause broadening and shifting of the energy levels of the molecule, and consequently modifies the conductance of an electrode–molecule–electrode junction. Díez-Pérez et al. demonstrated that this type of lateral coupling exists and can be controlled.[135] In their carefully designed experiment, changing the angle of the molecule from a highly tilted state to an orientation nearly perpendicular to the electrodes decreased the conductance by an order of magnitude, which agreed with the theoretical prediction. Lateral π orbital coupling can also exist between adjacent molecules. Although the importance of π–π overlap has long been recognized in thin-film organic electronics and supra-molecular chemistry, there exists no direct evidence to prove π–π stacking at the single molecular level. Wu et al. reported the use of oligo-phenylene ethynylene molecules as a model system, and demonstrated that aromatic π–π coupling between adjacent molecules was efficient enough to allow for the controlled formation of molecular bridges.[72] The experiment was carried out using a MCBJ in liquid at room temperature. With the molecules (one of the chemical linker groups was displaced or even fully removed to avoid

molecule–electrode bonding), a typical peak was still observed in the conductance histogram obtained during successive opening cycles. These experimental findings indicate that π–π stacking can be used as the dominant guiding force for the formation of molecular bridges and provides a strong basis for the design of future electromechanical and sensing devices that operate at the single-molecule level.

3.5. Electron Transport Mechanism Investigation

According to the characteristics of current-voltage dependencies, electron transport mechanisms are normally grouped into four groups: direct tunneling, field emission, hopping conduction, and thermionic emission.[41] Based on whether thermal activation is involved, the transport mechanisms fall into two distinct groups: (i) thermionic emission or hopping conduction, which show temperature-positive dependent I–V behavior; and (ii) direct tunneling or Fowler-Nordheim tunneling (field emission), which do not show temperature-dependent I–V behavior. Further analysis of the tunneling process can classify the mechanism as (1) sequential tunneling (incoherent tunneling) or (2) coherent tunneling.[133,136] In the sequential tunneling process, the electron tunnels from the source electrode to the molecule and then onto the drain electrode in a two-step process, which normally happens in long molecules with weak-coupling. In the strong-coupling regime, the electron effectively moves from the source to the drain without stopping on the molecules, and the current is always relatively weakly dependent on V_G.[96,137] MCBJ techniques enable to study not only the macro transport characterization but also the micro tunneling process. Here, we show a number of achievements related to the electron transport mechanism.

3.5.1. Transition Voltage Spectroscopy

Beebe et al. introduced the transition voltage spectroscopy (TVS) as an alternative method to characterize electron transport mechanisms. Based on a picture of a molecular junction as a tunnel barrier obeying the Simmons model for charge transport, they demonstrated that the metal–molecule–metal junction can exhibit current-voltage characteristics that correspond to a transition from direct tunneling to field emission as the applied bias exceeds a threshold voltage.[138] They proposed that the voltage at which the transition (V_T) occurs is proportional to the energy offset between the metal Fermi level and the nearest molecular orbital (MO). The promise of TVS is that molecular level positions can be roughly estimated in molecular junctions without applying extreme voltages. However, the interpretation of TVS is still under debate. In particular, a recent analysis of TVS shows that TVS is inconsistent with experimental data (such as the relation between V_T and electrode space d), also the linear correlation of the transition voltage with the energy offset was limited to a special transport model.[139,140] The possibility to accurately vary the funneling gap between the electrodes with MCBJ allows us to reveal the basic properties of TVS. Trouwborst et al. experimentally demonstrated that V_T has a week variation with the electrode spacing d in vacuum and TVS can be used as a characterization
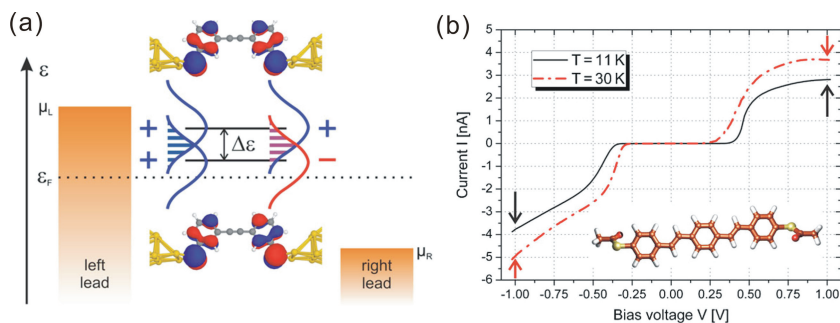
Figure 9. Evidence of vibrationally induced decoherence in single-molecule junctions. (a) Schematic representation of a single-molecule junction with two QDSs that are close in energy ($\Delta\varepsilon$) and different in their spatial symmetry. (b) I-V characteristics at different temperatures for single-molecule junction. Reproduced with permission.[95] Copyright 2012, American Physical Society.

tool for vacuum barriers.[141] Employing a MCBJ, we observed a V_T shift to a higher voltage in a single molecule junction as the gap size between two nanoelectrodes was reduced.[100] Several aspects (such as the transport model, electric field, and junction distortion) have to be considered for an explanation of the enhancement of field emission in single molecule junctions when intermolecular transport is unavailable.[138,139,142,143]

3.5.2. Vibrationally Induced Decoherence

Early charge transfer investigations focused mainly on the correlation between the chemical structure and transport properties. However, charge transport through molecular junctions is a quantum mechanical process, and quantum interference may exist in electron transport molecule junction.[1,144] In a purely electronic picture, destructive interference is an intrinsic property of many molecules.[144,145] Destructive interference occurs when the current is carried by quasi-degenerated electronic states, e.g., they differ in their spatial symmetry, as shown in **Figure 9**a. These quasi-degenerated states provide different pathways (that may be not spatially separated) for the electrons to tunnel through the molecular junction. Although their individual contribution to the current is substantial, their phase-corrected sum current may be very small. Electronic state interactions with vibrations may change this destructive interference significantly.[146] Consequently, destructive interference between the involved pathways may be quenched, which affects the electrical current. The vibration is strongly affected by the temperature, e.g., the vibration is weak at low temperatures. This rule means with decreasing temperature, destructive interference will continuously be reduced. Hence, for systems which exhibit destructive interference, a decrease in the electrical current with decreasing temperature is expected. Ballmann et al. analyzed decoherence effects in single-molecule junctions using the mechanically controlled break junction technique combined with density functional theory calculations.[95] In their experiment, molecules with electronic states close to the Fermi energy, generating vibration-sensitive interferences, showed strong temperature dependence on I/V characterization, as shown in Figure 9b. In contrast, molecules with electronic states located remotely from the Fermi

energy (a non-degenerate electronic state) showed temperature independent current responses. This is convincing evidence that decoherence resulting from coupling to vibrations plays an important role in single-molecule charge transport.

3.6. Control of Electron Transport Through a Single Molecule

Electron transport through a molecule may be controlled mechanically, electrostatically, magnetically, and electrochemically leading to various potential device applications. It is a challenging task to fabricate such gateable devices based on a two terminal device, but rapid advances have been made in recent years, especially when employing the MCBJ technique. The control of electron transport can be realized by several approaches, and many interesting phenomena have been observed.[36,64,103,147]

3.6.1. Gate Controlled Electron Transport

One approach to control the tunneling of electrons through molecules is the use of a gate electrode, which normally consists of a pair of electrodes (source and drain) together with a gate electrode on a solid substrate.[147] A large challenge is that screening by the charge rearrangements in the electrode always considerably weakens the gate effect in the nanometer-scale gate length. Therefore, to form single-molecule FETs, a gate electrode must be positioned in close proximity to the molecule junction. Gate modulation of single-molecule conductance has been demonstrated for various types of π-conjugated molecules.[147,148] Song et al. showed large modulation of I–V curves with the gate voltage in three terminal molecular junctions fabricated by the electromigration method.[63] The transition voltage spectroscopy derivation from the I–V curves indicated modulation of the energy gap due to the gate effect. Furthermore, feature peak height in IETS was found to be significantly enhanced when the gate voltage was increased. This demonstration validated the concept of molecular-orbital-modulated carrier transport, allowing new designs of molecular-based devices. However, fabrication of a molecule junction by electromigration techniques suffers from a relatively low yield, which may be improved by the MCBJ technique. Champagne et al. reported the implementation of both electrostatic gating and mechanical adjustability within a single-molecule device by means of an MCBJ.[103] They found that the threshold V required to overcome the Coulomb blockade depended on V_g, which shifts the energy of the molecular states with respect to the Fermi energy of the electrodes. At the same time, they found that mechanical stretch can change the slopes of the tunneling thresholds in the differential conductance map. This is a consequence of changes in the molecule–electrode capacitances, which affect the coupling efficiency between the molecule junction and the gate.

3.6.2. Mechanical Stretch Approach

By means of break junction techniques, it is possible to perform experiments that have no equivalent in conventional electronics. For instance, by applying a mechanical force to a molecular junction, it is possible to exploit the relationship between the electrical and mechanical properties of the molecule, which provides a method to control charge transport through the molecule junction. Bruot et al. reported on the variation of the electromechanical properties of a 1,4′-benzenedithiol molecular junction by stretching and compressing it.[143] They demonstrated that most of the conductance versus distance traces reach a plateau region with an increase in the conductance just before the complete break of the junction at low temperature. They attributed this finding to a strain-induced shift of the highest occupied molecular orbital towards the Fermi level of the electrodes, leading to a resonant enhancement of the conductance.[149] Similarly, we observed that the charge transport mechanism changed by applying a mechanical load to the molecular junctions for both CP-AFM and MCBJ experiments.[76,100] However, we attributed the change of the underlying mechanism partly to an enhanced electrical field effect and inter-molecule tunneling. Regardless, both the results from Bruot and our results indicate that electron transport is strongly sensitive to mechanically compressive or stretching loads, which provides an option to control electron transport characteristics in a mechanical way.

3.6.3. Control of Electron Spin

Typically, molecular-electronic experiments have focused on charge transport without taking the electron spin into consideration. Molecular devices may be well suited for applications requiring spin manipulation because of the relative weakness of the spin-orbit and hyperfine interactions in many molecules, which may help to isolate the spin from external degrees of freedom and preserve electron spin polarization over a much greater distance. Petta et al. studied the spin-polarized transport of electrons tunneling through a barrier consisting of a self-assembled octanethiol monolayer between two magnetic electrodes.[150] A striking finding was that a large variation of the resistance was observed as the magnetic field was swept through zero. This occurred because the magnetizations of the two electrodes underwent reversal processes at different fields close to the zero point, and they approached an approximately antiparallel configuration before ultimately aligning with the reversed field. During this process, the samples will exhibit clear changes in resistance.[151] Their measurements show that spin-conserving transport in molecular devices is possible at a low bias voltage. At high bias, tunneling via localized states under resonant conditions, which led to a change
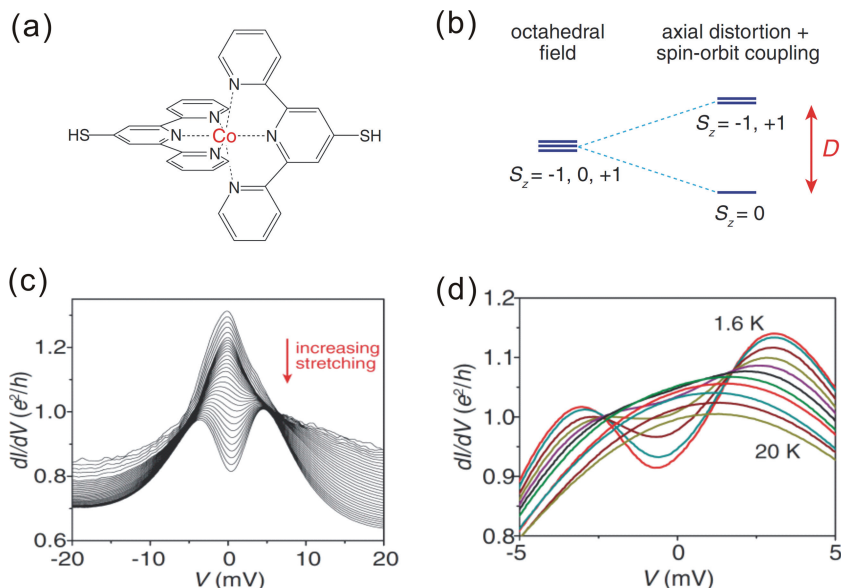

Figure 10. Mechanical Control of Spin States in Spin-1 Molecules. (a) Chemical structure of Co(tpy-SH)2, where tpy-SH is 4′-mercapto-2,2′:6′,2″-terpyridine. (b) Breaking of the degeneracy among the S = 1 triplet states by uniaxial distortion. (c) Line cuts showing dI/dV as a function of V for different values of molecular stretching at T = 1.6 K. (d) Temperature dependence of the conductance on the stretched side of the splitting transition. Reproduced with permission.[36] Copyright 2010, AAAS.

of the effective spin polarization of electrons, was reported by Tsymbal et al.[152] At low temperature, a spin-singlet state may be formed from a localized spin-1/2 electron and the delocalized Fermi sea, leading to zero-bias conductance (Kondo effect) as discussed above. With C_{60}, which possesses an unpaired spin in equilibrium, Parks et al. successfully tuned the Kondo effect with a MCBJ.[153] By precisely varying the electrode spacing, they were able to change both the width and height of the Kondo resonance, offering an approach to control electron transport through unpaired spin molecules. Later, Parks et al. demonstrated mechanical control of spin states in spin-1 molecules.[36] They reported that molecular spin states and magnetic anisotropy can be manipulated in the absence of a magnetic field just by modification of the molecular symmetry. In the experiment, they controllably stretched individual cobalt complexes having large magnetic moments (spin S = 1) to modify the molecular symmetry, and simultaneously measured current flow through the molecule. **Figure 10a** shows the chemical structure of the investigated molecular (Co(typ-SH)2 complex. As a molecule was stretched, the single conductance peak split into two beyond a value, as shown in Figure 10b. On a stretched molecule junction with fixed electrode spacing, the temperature dependence of the conductance also showed a splitting behavior, as shown in Figure 10c. The corresponding interpretation for this observation is shown in Figure 10d. For a unstretched S = 1 ion in a ligand field with octahedral symmetry, the triplet states are strictly degenerated. However, if the molecule is stretched and distorted, the $S_z = 0$ state will be lowered by a splitting energy D below the $S_z = \pm 1$ states, corresponding to uniaxial spin anisotropy. This broken degeneracy quenches the Kondo resonance near zero bias and causes

conductance peaks at V = ±D/e due to inelastic tunneling. Their findings demonstrate a mechanism of spin control in a single-molecule junction, and more single-molecule spin electronics studies are anticipated.

3.7. MCBJs Combined with Other Techniques

3.7.1. MCBJ-Transmission Electron Microscopy

As the scale of microelectronic engineering continues to shrink, interest has been focused on the nature of electron transport through essentially nanometer scale channels, such as quantum wires.[154] However, it is a large challenge to simultaneously obtain both an atomic-scale structure and electron transport properties. Due to the small and flexible size of the MCBJ setup, MCBJs can be integrated into a transmission electron microscopy (TEM) setup, which is an appropriate way to handle the challenge.[155–158]

Using in situ high resolution transmission electron microscopy, Rodrigues et al. have studied atomic arrangement and defect formation in metal nanowires (NWs) generated by mechanical elongation.[156] In their experiment, a time-resolved high resolution transmission electron microscope was used to study metal NW atomic arrangements. The sample consisted of a self-supported polycrystalline thin metal film (3–4 nm thick), which was perforated at several points by focusing the microscope electron beam until a nanometric bridge was formed between two holes. The electron beam was then turned to its image state, and time-resolved atomic resolution images were recorded during the elongation process. For example, **Figure 11** shows snapshots of a platinum NW formed along the [111] direction.[156] It was observed that the narrowest constriction of gold and platinum NWs was crystalline and defect-free, and gold NWs adopted only three types of atomic arrangements. Atomic arrangements and quantum conductance of silver nanowires generated by mechanical elongation was also investigated.[155] The surface properties of Ag induced unexpected structural properties; for example, a predominance of high aspect-ratio rod like wires was obtained. These results emphasize that the conductance of metal point contacts is determined by the preferred atomic structures and that atomistic descriptions are essential to interpret the quantum transport behavior of metal nanostructures. Lagos et al. further studied the influence of thermal effects on the structural and transport response

of atomic-sized Ag nanowires and combined time-resolved atomic resolution TEM with ultra-high-vacuum mechanically controllable break junctions.[157,158] They revealed that it was extremely difficult to compare nanowire conductance experiments performed at different temperatures due to fundamental modifications of the mechanical behavior. All the experiments mentioned above were performed without bridged molecules. With the development of TEM technology in the future, electron transport through a molecule junction could be measured as TEM images of the molecular junction are simultaneously taken. It would be an amazing possibility for examination of the relationship between geometric information and electronic transport properties.

3.7.2. MCBJ-Surface Enhanced Raman Spectroscopy

Electronic transport through single molecules is affected by the molecular electronic structure as well as the vibration mode (chemical information), which is extremely difficult to assess by standard voltage-current measurements. Surface-enhanced Raman scattering (SERS) is a powerful tool to independently investigate the vibration mode of the molecule structure. A large step was made by Ward et al., who reported simultaneous measurements of the conductance and the Raman spectra of molecular junctions formed by the electron migration method.[58] However, the gap size formed by the electron migration method cannot be continuously adjusted, which limited the junction yield. According to SERS theory, the excitation of surface plasmons around the metal is sensitive to the shape of the nanoparticle and the distance of the nanoparticle (nanoelectrode). Unfortunately, the dependence on the separation between two nanoparticles has hardly been realized experimentally because there are few methods capable of precisely and flexibly adjusting nanoparticle separation during SERS measurement.[159] Tian et al. reported a combined SERS and mechanically controllable break-junction (MCBJ) method to measure SERS signals of molecules located inside the nanogap between two electrodes on a Si chip.[159] Their MCBJ chips were micro-fabricated with gold wire on a Si substrate using optical lithography, and the gap between the electrodes was reduced from approximately 1 μm to 1 nm or less by electrochemical deposition.[87] The gap was controlled mechanically using a piezoelectric transducer with sub-angstrom resolution.[86,97,105] An incident laser was focused onto the molecular junction via a lens from the top of the MCBJ chip, and the scattered light was collected with the same lens, as shown in **Figure 12**. They demonstrated that the SERS intensity of sample molecules depends on the gap width and the incident light polarization, indicating that the signals came from the molecules inside the gap. The SERS-MCBJ method shows potential as a powerful characterization tool for molecular electronic studies, both physically and chemically. Combined with electrical measurements, one can answer questions such as if and how a molecule is present between two probing electrodes. However, the collected signal might be a superposition from hundreds or thousands
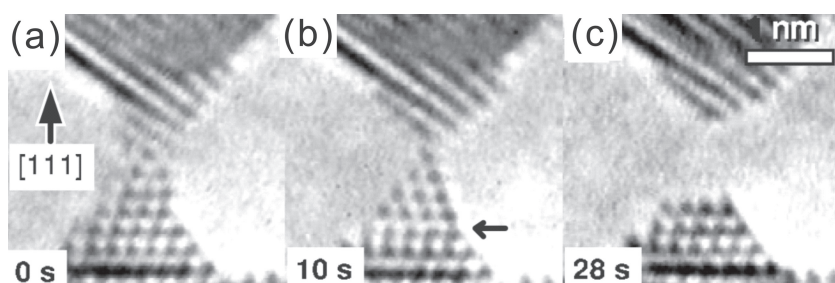
Figure 11. The images obtained by TEM combined with the mechanically controllable break junction technique. (a–c) High resolution TEM snapshots of a time evolution of a platinum nano wire formed along the [111] axis.
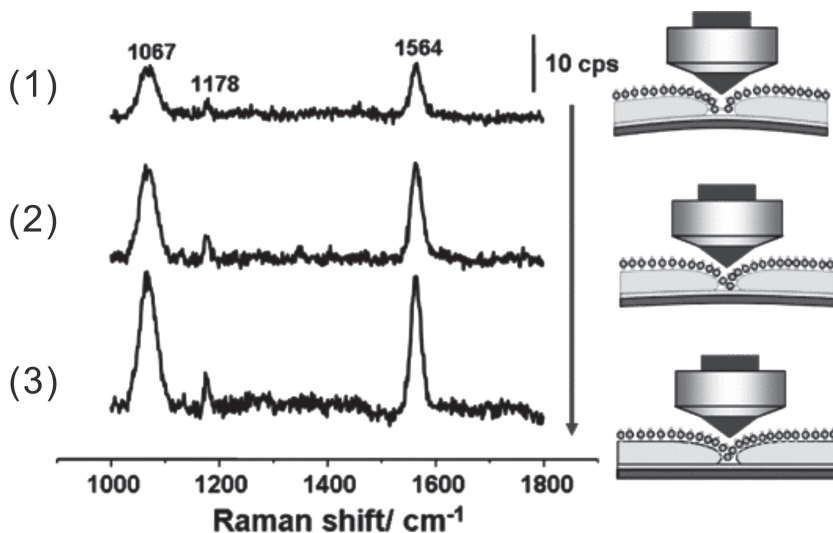
Materials
Views
www.MaterialsViews.com

**ADVANCED
MATERIALS**
www.advmat.de

REVIEW

Figure 12. Mechanically controllable break junction technique combined with surface enhanced Raman spectroscopy technique. SERS of 1,4-benzenedithiol in the nanogap with the process of bending the metallic electrodes pair. The gap width is reduced, from (a) 8 Å, (b) 6 Å, to (c) 4 Å and the increased intensity of the signal is observed. Laser: 632.8 nm. Reproduced with permission.[159] Copyright 2006, American Chemical Society.

of molecules in the vicinity of the electrode bridging molecule. Therefore, it remains a challenge for SERS to eliminate the influence of the surrounding molecules on the signal from the metal–molecule–metal junctions.

3.7.3. MCBJ-Inelastic Tunneling Spectroscopy

Recently, inelastic tunneling spectroscopy (IETS) emerged as one of the premier characterization methods for single molecules. Considering a phonon of energy ω with electron–phonon coupling, once the voltage applied to the junction reaches a threshold of $V_\omega = \omega/e$, it is possible for an electron to excite the phonon mode when tunneling through the junction. This process opens an additional transmission channel when the bias is above the threshold voltage V_ω, leading to an increase in the total conductance where non-linearity of the I-V characteristic is expected. However, the nonlinearity in the current typically only possesses a small slope change in the I-V characteristic. Therefore, it is more common to measure the differential conductance (dI/dV vs. V) curve, thus allowing one to observe steps at V_ω where one phonon mode is activated. If one takes the second derivative of the current ($d^2I/dV_{2 vs.}$ vs. V), exactly as in IETS, a peak would be observed at Vω. A series of peaks can be observed if more than just electron–phonon coupling (interaction between electrons and molecular vibrations) modes exist. Therefore, IETS is very suitable for detecting vibrational excitations and is sensitive to contact geometry and molecular conformation. A detailed introduction of IETS can be found in the review paper.[160]

A few pioneering scientists have successfully combined MCBJ and IETS techniques to obtain fingerprint information of different molecules.[90,161–163] Taniguchi et al. combined analyses of single-molecule conductance and inelastic electron tunneling spectra and found that the peak line width of the inelastic

electron tunneling spectrum decreased as the modulation voltage and temperature were decreased.[162] Fock et al. reported on the vibrational fingerprint of single C_{60} terminated molecules in a mechanically controlled break junction (MCBJ) setup to address different molecular configurations.[161] They found that the vibrations of the anchoring C_{60} dominated the IETS spectra, which may mask vibration modes from other parts of the molecule. However, they found a way to identify the additional modes from the fluorine backbone by the addition of infrared (IR) and Raman spectroscopy. Their experiments indicated that it is possible and necessary to combine several different techniques to reveal detailed information regarding the molecules.

Figure 13 shows the IETS of 1,6-hexanedithiol (HDT) in different molecular conformations, as reported by Kim et al.[163] With the MCBJ technique, they can identify the high conductance state and low conductance state, which correspond to two different molecular conformations, as shown in Figure 13d. Two completely different IETS were observed at the low conductance state and high conductance states, as shown in Figure 13(a,b). A gentle mechanical stretch also led to a small change of IFTS, which reflected a change of electron density during the stretch period. The red shift of the ν(C-S), as shown in Figure 13c, could have been caused by the reduction of the electron density in C-S bonding, due to the weaker overlap of the orbital. Moreover, they used two different electrode materials to distinguish the contact geometry by IETS. They successfully demonstrated that combining inelastic-electron-tunneling spectroscopy with mechanical control and electrode material variation (Au or Pt) enables the influences of contact geometry and molecular conformation to be separated.

3.7.4. MCBJ- Noise Spectroscopy

Noise characterization is a key issue for any type of nanodevice, including those based on single molecules, because it influences the performance and the reliability of the devices. In addition, it gives insight into time-dependent physical phenomena and is inherently linked to the charge transport characteristics of the investigated system. Concerning monolayer junctions, random telegraph noise was observed above the $1/f$ noise in alkyl-based metal/multi-molecule/metal junctions at high bias voltages and was attributed to a trapping-detrapping process via localized energy states.[164] This finding demonstrated that noise characterizations can be used for evaluating the influence of localized states on charge transport in molecular junctions. The noise characteristics of bare nanocontacts in a MCBJ without molecules was systematically investigated by Wu et al.[165] They demonstrated that, as a function R, the normalized noise S_V/V^2 showed a pronounced crossover from $\propto R^3$ for low-ohmic junctions to $\propto R^{1.5}$ for high-Ohmic junctions. S_V is the voltage noise power spectral density, V is the
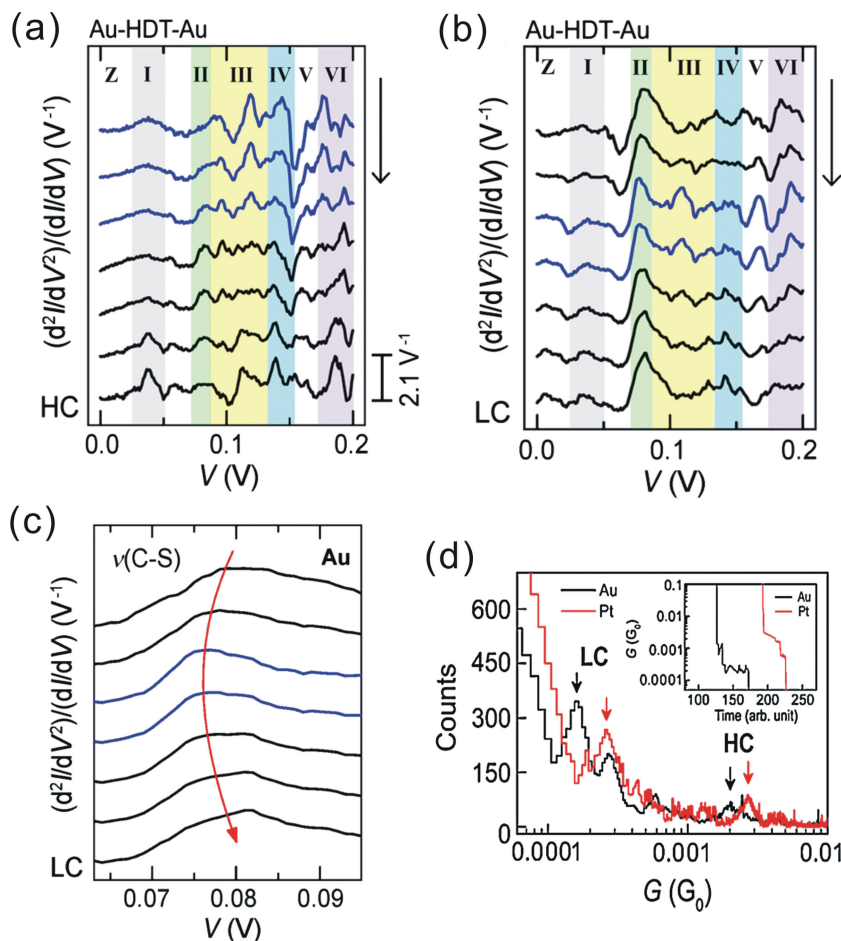
Figure 13. Inelastic tunneling spectroscopy (IETS) obtained with a mechanically controllable break junction. IETS in the high conductance (HC) and the low conductance (LC) regimes, displaced vertically in the order of the junction distances in the Au-HDT-Au junction. The IETS are measured from a distance of 0.5 (top) to 4.5 Å (bottom) for the HC regime (a) and between 5 (top) and 14 Å (bottom) for the LC regime (b). (c) Enlarged vibration mode reported in (b). (d) Histograms of Au (black) and Pt (red) junctions, respectively. Inset: Representative conductance traces. Reproduced with permission.[163] Copyright 2011, American Physical Society.

only in the amplitude but also in the exponent of the power law, were observed in their MCBJ experiments. Possible mechanisms are further discussed, for instance, molecule structure fluctuation, and gold–molecule contact and instabilities of electrode atoms. We measured and compared both molecule-free and single-molecule containing mechanically controllable break junctions.[167] Both junctions demonstrated $1/f$ noise characteristics, and an additional $1/f^2$ noise component was clearly revealed when a single molecule bridged the nanoelectrodes, as shown in **Figure 14**a. Moreover, a linear dependence of the current in the small current regime was observed. The recorded $1/f^2$ electric noise component relative to a single bridging molecule was interpreted as a manifestation of a dynamic reconfiguration of molecular coupling to the metal electrodes during current flow. The reconfiguration changes occurred without complete bond breaking and involved near-configuration states with very similar electric properties, which agrees with Secker analysis.[168]

It is evident that for molecules, any change of the geometric structure leads to a change of the electronic structure, and vice versa. Secker demonstrated how this affects the transport characteristics by simultaneous measurement of the conductance and noise level.[94,168] Interestingly, they observed that the maximum of noise was actually at a lower bias than the maximum of the conductance peak. In other words, the fluctuations were maximized when the current started to flow. The observation that the noise peak lies before the conductance maximum can be understood in this way: when electron
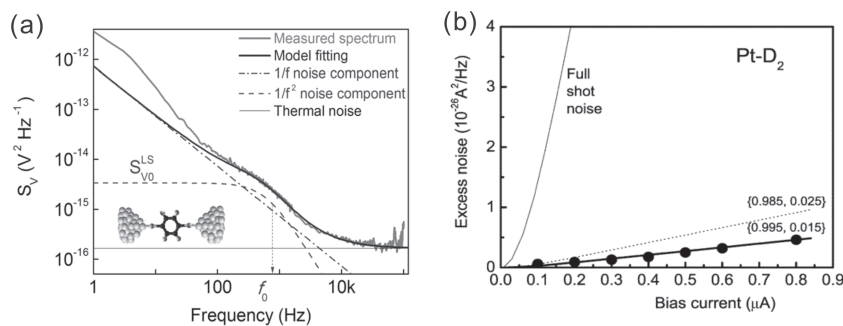
applied voltage, and R is the resistance of the nanocontact. The measured powers of 3 and 1.5 are in agreement with $1/f$ noise generated in the bulk and reflect the transition from diffusive to ballistic transport.

MCBJs can be conveniently used to investigate the noise characteristic after integrating individual molecules into the nanocontact due to the high intrinsic stability and the tunability of the gap size. Ochs et al. reported on frequency-dependent measurements within the electrical current through single-molecule junctions at cryogenic temperatures in a frequency range of 100 Hz to 100 kHz.[166] The data showed a power-law decrease of noise towards high frequencies, which could be related to fluctuating degrees of freedom of the microscopic configurations in the junction. Sample-to-sample fluctuations, not

Figure 14. MCBJ combined with noise spectroscopy. (a) The voltage noise power spectral density of the molecule-containing junction in the lock-in state, corresponding to a single BDA junction. The fitting curve is the superposition of $1/f$, $1/f^2$ and thermal noise components shown by a dash-dotted line, dashed curve, and thin gray line, respectively. Reproduced with permission.[167] Copyright 2012, The American Institute of Physics. (b) Excess noise (the difference between the measured white noise level with and without current) as a function of the applied current for a Pt-D2-Pt junction. The Poissonian shot noise level is indicated by "full shot noise". A strong quantum suppression of the noise was observed. Reproduced with permission.[171] Copyright 2006, American Chemical Society.

tunneling is hindered by a poor overlap of local orbitals (Franck-Condon blockade), vibrations may increase the current and lead to a nonlinear amplification of both the current and further vibrations, resulting in sudden current bursts.[169]

Molecular-vibration-induced current noise can be used as signature for single-molecule identifications. In a study by Tsutsui et al., both the electric current noise and IETS of Au/hexanedithiol/Au single-molecule junctions were measured.[170] They found increased current oscillations synchronous to electric field excitations of specific molecular vibrational modes active in the electron-phonon interaction. This finding unambiguously indicated that the voltage-dependent electric noise stems from inelastic interactions between electrons and molecular vibrations, which thereby enable single molecule fingerprinting through examination of the noise spectra[160,170]

Shot noise can be used to examine the transmitting channels as well. Shot noise results from the discrete nature of the electronic charge. Djukic et al. reported measurements of shot noise in the current through a single D_2 molecule in cryogenic temperatures.[171] After dropping the low-frequency portion dominated by 1/f-noise, compensating for the roll-off and subtracting the thermal noise for a series of bias currents on a given contact, they obtained the dependence of the excess noise as a function of applied bias, as shown in Figure 14b. At the same time, the conductance for such a junction at zero bias was measured and compared with the conductance expression. They found that the noise increased as soon as the transmission of the almost fully open channel was reduced. This sensitivity is illustrated in Figure 14b. The observed quantum suppression shows that conductance is carried dominantly by a single, almost fully transparent conductance channel. Shot noise suppression in atomic-scale Au junctions at room temperature was also observed by Wheeler et al.[172] Using a high-frequency technique, they simultaneously acquired noise data and conductance histograms of an Au junction under ambient conditions. The presence of noise suppression at room temperature explicitly demonstrates the quantum character of transport in these atomic-scale devices. Inelastic processes, such as electron-phonon scattering, can remove energy from the "hot" electron system and redistribute electrons between the different quantum channels. This is what causes the suppression of shot noise in macroscopic conductors at room temperature.

3.8. Additional Applications

Beyond the application of molecular electronics, MCBJ can be applied to other areas, for instance, atomic contact formation, a metal atom switch, semiconductor materials, and microfluidic nanoparticles. Here we just select a few examples, related to molecular electronics, to show the wide application of MCBJ techniques.

3.8.1. Metal Wire Quantum Properties

The investigation of quantum effects on electron transport has attracted much interest. Quantum properties of conductance can be observed when 'breaking' a metallic contact: as two metal electrodes in contact are slowly separated, the contact

area undergoes structural rearrangements until it consists of only a few bridging atoms in its final stages. Just before the abrupt transition to tunneling occurs, the electrical conductance through a monovalent metal contact is always close to a value of $2e^2/h$, where e is the charge of an electron, and h is Planck's constant. This value corresponds to one quantum unit of conductance, indicating that the contact consists of a single atom. In 1998, Scheer et al. obtained one atomic constrictions for four different metallic elements (Pb, Al, Nb and Au) with both STM and MCBJ techniques.[32] In same year, Yanson et al. demonstrated that four peaks could be clearly observed in the histogram of the length distribution for the last plateau, which indicated gold chains with a one-atom thickness and at least four atoms in length can be obtained at 4.2 K during the breakage of atomic-scale gold contacts.[33]

However, there were strong arguments with respect to the physical interpretation of the conductance steps of approximately $2e^2/h$ that appeared during the nanowire elongation process.[31,80,155,173,174] One opinion attributed the conductance steps to conductance quantization (electron channels). Another opinion attributed the conductance steps to discrete contact size changes (rearrangement of the atom). In fact, it has been extremely difficult to discriminate between structural and electronic effects in the nanowire elongation experiment with MCBJs because both are simultaneously modified during the measurement.[155] In 1995, Krans et al. used the fact that the degeneracy of conduction modes of a three-dimensional point contact should result in a characteristic sequence of conductance values to distinguish the effects of conductance quantized from those of discrete variations in contact size in the break junction experiment, confirming that conductance quantization did indeed occur.[174] A detailed discussion concerning the quantum properties of atomic-sized conductors can be found in the literature.[175]

3.8.2. Metal Atomic Switch

Martin et al. have exploited the electromechanical properties of single-atom relays and the corresponding switch behavior with gated mechanical break junctions. The gate voltage can be used to reversibly switch between a monatomic contact, with a conductance of approximately $2e^2/h$, and the tunneling regime.[176] Devices on phosphor bronze wafers were fabricated by a two-step lithography process. The device fabrication was completed by dry etching in reactive ion plasma to remove the sacrificial layer between the gate and the source-drain electrodes, leading to a suspended gold bridge, as depicted in **Figure 15**a. The gate potential could control the breaking and formation of the Au–Au bond and switch the source-drain conductance, as shown in Figure 15b. They also demonstrated that the source-drain conductance varied smoothly with gate voltage in the tunneling regime. They put forward a continuum model to analyze the results. In brief, the electrostatic attraction of the suspended electrodes and gate electrode led to tip deflection and gap size variation between the source-drain electrodes. In contrast to silicon-based gated MCBJs, the devices fabricated with phosphor bronze possessed sufficient flexibility to vary the electrode spacing over several nanometers. However, the observed electromechanical deflection of the tip and corresponding gap size
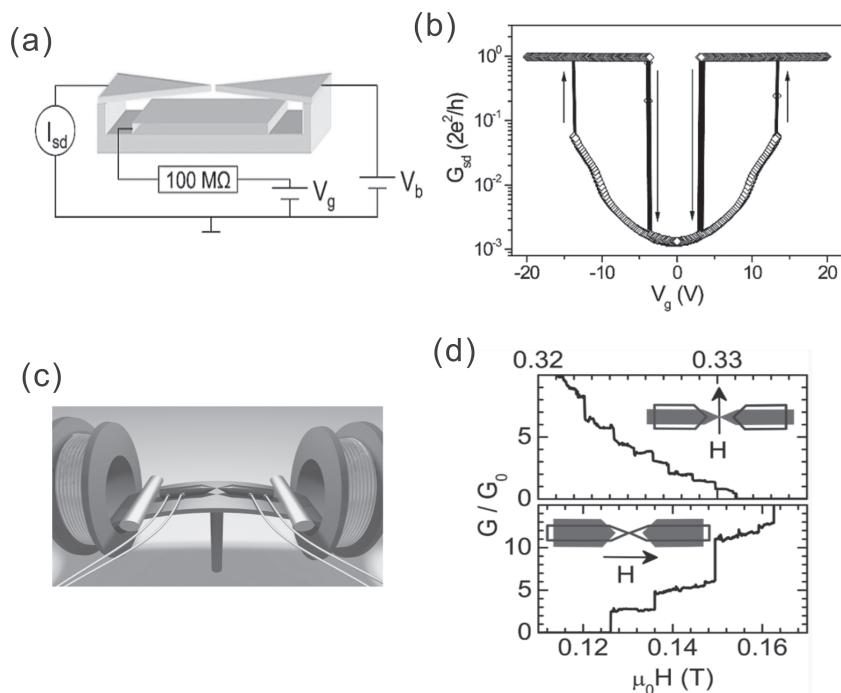
Figure 15. Atom switch. (a,b) Gate-induced reversible switching of single-atom contacts in mechanical break junctions. (a) Schematical draw of the electrical measurement circuit. (b) Switching characteristics, in which bare metal bridge is established at high gate voltages. Reproduced with permission.[176] Copyright 2009, American Chemical Society. (c,d) Switching the conductance of Dy nanocontacts by magnetostriction. (c) Schematic of magnetic field control set up. (d) The conductance can be changed reproducibly by variation of the magnetic field H. Reproduced with permission.[178] Copyright 2011, American Chemical Society.

substrate, as shown in Figure 15c. The discrete changes in G (H) in the range of several $G_0 = 2e^2/h$, as shown in Figure 15d, was attributed to the magnetostriction.[178] This realization of a magnetostrictive few-atom switch demonstrates the possibility of reproducibly tuning the conductance of magnetic nanocontacts with a magnetic field.

3.8.3. Micro-Fluid Channel

Tsutsui et al. reported the development of a microfluidics-integrated mechanically controllable break junction device and its application to electrical characterization of DNA-sized particle dynamics in a microfluidic channel.[179] Scanning electron micrograph images of the microfluidics-MCBJ device are presented in **Figure 16**a. The device consisted of free-standing Au nanojunctions embedded in a fluidic channel, see Figure 16b. After the gap was adjusted to a specific size, a constant DC bias voltage of V_e was applied between E_1 and E_2 to cause Au nano particles to flow through the microfluidic channel. Schematic drawing of particle pass through microfluidic channel was presented in Figure 16c. Simultaneously, a current across the nanogap electrodes (I) was recorded under a DC bias voltage of V_b. Figure 16d shows the I–t curves acquired under various environments. In a vacuum, the current was quite stable. When measured in the particle solution, both the current and noise increased proportionally to the particle concentration. This manifests the ionic nature of the Au nanoparticles used – the larger leakage current

variation with gating imposed limitations for molecule investigation. Two possible strategies can be employed to meet the challenge. The first approach, which they mentioned in their paper, is to increase the electrode rigidity.[177] An alternative approach is fabrication of a side gate electrode instead of a bottom electrode, with the side gating configuration the deflection of the tip is dramatically suppressed.[100,106,167]

The electrical conductance switch behavior of mechanical break-junctions fabricated from the rare-earth metal dysprosium has been investigated by Müller et al.[178] During the mechanical breakage of the wire, the conductance was reproducibly changed by variation of the magnetic field H, due to the large magnetostriction of Dy. In their experiments, thin wires cut from bulk Dy polycrystals in the ferromagnetic state were used. A notch was mechanically made in the middle of the wire, which is where the sample broke during bending. The wire was then glued to a flexible copper-bronze substrate coated with a 2 μm thick insulation film. The sample was mounted into a mechanically controlled break-junction device and cooled to 4.2 K. The magnetic field was provided by a superconducting Helmholtz coil in the plane of the
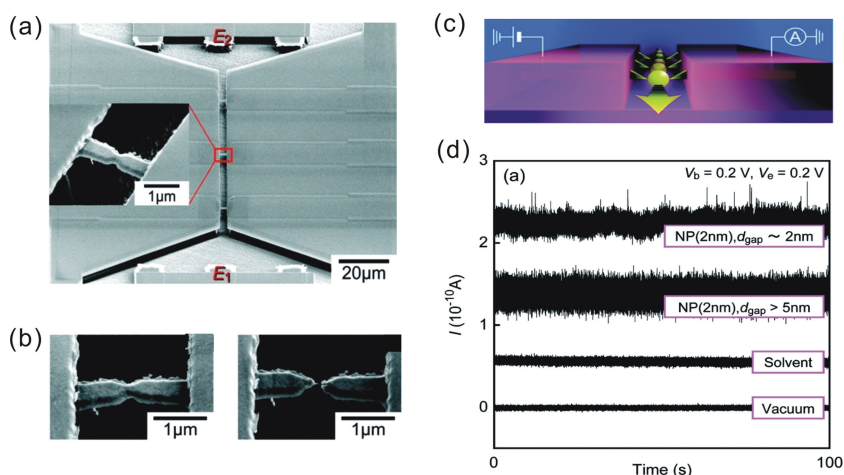

Figure 16. Microfluidics-integrated mechanically controllable break junction. (a) Scanning electron microscopy images of the microfluidics-integrated MCBJ device showing three Au nanobridge electrodes. Inset is a magnified view showing the free-standing configuration of the Au junction. (b) A nanojunction before and after mechanical breaking. (c) Schematic of DNA-sized particle dynamics in a microfluidic channel. (d) I-t curves measured under various environments. Reproduced with permission.[179] Copyright 2009, American Chemical Society.

associated with high ion (nanoparticles) content. Moreover, with an appropriate gap size, pulse-like signals were detected, which were attributed to particle translocation through the electrode gap region. This provides a method to detect the transport speed of nanoparticles. They also found that the high electric field between the nanogaps and the corresponding high electrostatic electrode–particle interaction could slow down the particle flow through the electrode nanogaps. The results suggest the useful capability of a transverse electric field for controlling DNA translocations through a nanopore or nanochannel.

4. Conclusion and Outlook

Molecular electronics is an interesting topic which facilitates the understanding of fundamental aspects of the charge transport through individual molecules or monolayers, and which has brought together scientists from different disciplines, including physicists, chemists, and engineers. The rapid growth of molecular electronics and research on molecular junctions have yielded new phenomena and devices with possible vast applications.[8] Further work is required before molecular junctions are fully understood and applicable in commercially viable manifestations. A proposed road map to meet the experimental challenges in the design and fabrication for molecular electronics can be found in a previous review paper.[12]

It is worth noting that during the last several years, the techniques for the fabrication of MCBJ setups and chips have made great progress, which will tremendously extend its potential applications. With advanced fabrication and measurement techniques, MCBJ experiments can be conducted under ambient and cryogenic vacuum conditions, in solvents, and even under electrochemical potential control.[36,180] The bandwidth of the measurement electronics has been optimized to enable fast dI/dV spectroscopy of molecular junctions, even at extremely low current.[180,181] Target molecules, ranging from simple dielectric model molecules via molecular diode to molecular switches, transistors, and molecular motor prototype bio-functional molecules, have been integrated into MCBJs, which can be investigated by multi-terminal devices. The MCBJ technique, with unique mechanical stability, has progressed rapidly from both the scientific and technological viewpoints, encouraging further advances in single-molecule electronics. The significant achievements discussed in this review are just a small fraction of the tremendous advances achieved so far. There are still key issues that need to be resolved and deserve further investigation, some of which are discussed below.

1. Substrates: Typically, three types of substrates are used in MCBJ chip fabrication: silicon, bronze, and spring steel. The fragile silicon wafer cannot be deeply bent, leading to a limited gap size between the electrodes. To support the breaking process, the electromigration approach can be used to assist breaking of the metal wire.[103] An alternate method to get around the bending limits of silicon substrate is using silicon membranes rather than silicon wafers.[182] Concerning spring steel and bronze substrates, polymer layers (mainly polyimide) have been used to insulate the electrodes from the substrate. However, the deformation of the polyimide layer upon different temperatures can lead to gap size variation.[95] Therefore, it is necessary to find an appropriate substrate to maintain thermal stability and unlimited gap size. We examined using Si_3N_4 as an insulating layer and found that it is an alternative material to maintain both thermal stability and flexibility.

2. Integration: Although the MCBJ technique is very useful for fundamental investigation and can be easily combined with other techniques, it is not facile to fabricate highly integrated molecular commercial devices because of the constraint of the push rod components. Piezoelectric components of small size usually only supply short displacement for the push rod, which will lead to limited gap size variation. If one tries to obtain a larger gap size by sacrificing the attenuation factor, one may lose mechanical stability. That means one has to maintain a balance between the mechanical stability and the available gap size. Chip architectures using flexible materials as sample substrates, such as hardened polyimide without solid support, may help to minimize the demission of MCBJ devices. Beyond this method, the discovery of a new architecture not limited to a three point apparatus with a novel miniaturized push rod, which can also bear cryogenic temperatures as well as high temperatures, may pave the road from fundamental research to application related research. It has been reported that a micrometer-scale motor has been put into use, which may be employed as a potential push rod in the future.

3. Leads: Precise control of the contact geometry down to the atomic scale has been a difficult challenge. A widely employed method for MCBJs is to attach molecules terminated with thiol groups to gold electrodes. This approach has many advantages but also suffers from undesired effects, such as high metal-atom mobility at room temperature and a large polarization field at the metal-molecule interface.[183] There are reports that have looked into novel contacts, such as C-Si and C-Au bonding.[184] With electron beam lithography, it is possible to fabricate suspended silicon electrodes in MCBJ chips. By bridging the molecule between highly doped silicon electrodes and forming silicon-molecule-metal, we are convinced that new phenomena can be observed.[185] Compared with metal wires, carbon nanotubes possess high conductivity, better defined contact configurations, and better contact to organic molecules via C-–C bonding. Moreover, nanotube electrodes can reduce electric field screening, which strongly occurs in gold electrodes, and will increase the gate coupling efficiency in three terminal devices.[160] The challenge for this application is to precisely control the growth of carbon nanotubes at desired sites with the desired structure and orientation. Tsutsui et al. reported electrical break down of carbon nanotubes with MCBJ techniques.[186] Graphene possesses several advantageous characteristics, including low sheet resistance, high optical transparency, high electron mobility, zero energy gap and excellent mechanical properties.[187] If one succeeds in reproducibly bridging nanotube fragments or graphene with individual molecules,[62] the advantages of MCBJs and graphene could be combined, and junctions could be created from fully assembled molecular building blocks.

4. Additional topic: There are several potential research topics deserving further study using MCBJs. For example, 1) due

to the fact that we can precisely control the separation of two electrodes with MCBJs, we can accurately measure the lifetime of a single-molecule junction before breakdown during the stretch process. The measurement of lifetime during a negligible mechanical stretch process enables us to extract the local temperature based on thermodynamic bond-breaking theory.[188] 2) A single molecule can be easily sandwiched between two symmetric atomic scale tips, without parallel molecules, using a MCBJ. Therefore, we can investigate the interference between two different transport paths within a single molecule, which strongly affects molecular conductance and even the transport mechanism.[95,144] A case in point of this is that the conductance superposition law for parallel components within a single molecule can be addressed.[24] 3) Although different types of gate electrodes have been employed in MCBJs, such as a bottom gate to control the electron transport through molecule junctions, electron transport through the molecule may be controlled by a more general gate electrode, including electrical gates, magnetic gates, optical gates, mechanical gates, and electrochemical gates. The simple system of MCBJs facilitates the integration of different types of gate electrodes, leading to various potential research topics and device applications.

5. Modeling: Recently, considerable theoretical calculation results have been reported, but the theoretical developments are mostly beyond the scope of this review. For a theoretical overview of the electronic transport in molecular junctions, please refer to previous papers.[11,149,189] Here, we present a few examples of the theoretical achievements related to MCBJs: Wang et al. simulated how a metal wire break occurs using a MCBJ, and detailed information concerning atom re-arrangement during the break process was revealed;[190] Lin et al. compared the advantages and disadvantages between MCBJs and electron migration junctions with non-equilibrium Greens function and density functional theory approaches;[191] French et al. demonstrated the utility of an updated simulation method that allowed for the incorporation of important environmental factors into simulations of the formation of molecular junctions. With respect to electron transport through a molecular junction, the Landauer formula, Breit-Wigner formula, Simmons model and others have been put forward.[41,192] On the one hand, theoretical calculation promotes the development of experiments by predicting, confirming and interpreting the experimental phenomenon. On the other hand, the progress in experimental research also poses new challenges to theoretical and computational methods. Density functional theory is well established, and the limits of its validity are well known when applied to bulk metallic systems, as well as to organic molecules in isolation.[189,193] Development of theories that include realistic molecules, electrodes, molecule–electrode interfaces, electron–vibration, electron–phonon interactions, spin–orbit interactions, and electron–solvent couplings will be critical in the future.[11]

Acknowledgements

[1] D. Fracasso, H. Valkenier, J. C. Hummelen, G. C. Solomon, R. C. Chiechi, *J. Am. Chem. Soc.* **2011**, *133*, 9556.

[2] S. J. van der Molen, P. Liljeroth, *J. Phys.: Condens. Matter.* **2010**, *22*, 133001.

[3] F. Chen, J. Hihath, Z. F. Huang, X. L. Li, N. J. Tao, *Annu. Rev. Phys. Chem.* **2007**, *58*, 535.

[4] A. Coskun, J. M. Spruell, G. Barin, W. R. Dichtel, A. H. Flood, Y. Y. Botros, J. F. Stoddart, *Chem. Soc. Rev.* **2012**, *41*, 4827.

[5] A. Aviram, M. A. Ratner, *Bull. Am. Phys. Soc.* **1974**, *19*, 341.

[6] H. Song, M. A. Reed, T. Lee, *Adv. Mater.* **2011**, *23*, 1583.

[7] E. Lörtscher, B. Gotsmann, Y. Lee, L. P. Yu, C. Rettner, H. Riel, *ACS Nano* **2012**, *6*, 4931.

[8] L. C. Cao, S. Y. Chen, D. C. Wei, Y. Q. Liu, L. Fu, G. Yu, H. M. Liu, X. Y. Liu, D. X. Wu, *J. Mater. Chem.* **2010**, *20*, 2305.

[9] J. S. Lindsey, D. F. Bocian, *Acc. Chem. Res.* **2011**, *44*, 638.

[10] T. Li, W. P. Hu, D. B. Zhu, *Adv. Mater.* **2010**, *22*, 286.

[11] S. M. Lindsay, M. A. Ratner, *Adv. Mater.* **2007**, *19*, 23.

[12] R. L. McCreery, A. J. Bergren, *Adv. Mater.* **2009**, *21*, 4303.

[13] a) F. Anariba, R. L. McCreery, *J. Phys. Chem. B* **2002**, *106*, 10355; b) H. J. Yan, A. J. Bergren, R. L. McCreery, *J. Am. Chem. Soc.* **2011**, *133*, 19168.

[14] a) J. Puigmarti-Luis, A. Minoia, S. B. Lei, V. Geskin, B. Li, R. Lazzaroni, S. De Feyter, D. B. Amabilino, *Chem. Sci.* **2011**, *2*, 1945; b) H. P. Yoon, M. M. Maitani, O. M. Cabarcos, L. T. Cai, T. S. Mayer, D. L. Allara, *Nano Lett.* **2010**, *10*, 2897.

[15] E. Adaligil, K. Slowinski, *J. Electroanal. Chem.* **2010**, *649*, 142.

[16] R. C. Chiechi, E. A. Weiss, M. D. Dickey, G. M. Whitesides, *Angew. Chem. Int Ed.* **2008**, *47*, 142.

[17] M. M. Thuo, W. F. Reus, C. A. Nijhuis, J. R. Barber, C. Kim, M. D. Schulz, G. M. Whitesides, *J. Am. Chem. Soc.* **2011**, *133*, 2962.

[18] J. Chen, M. A. Reed, A. M. Rawlett, J. M. Tour, *Science* **1999**, *286*, 1550.

[19] M. Tsutsui, S. Rahong, Y. Iizumi, T. Okazaki, M. Taniguchi, T. Kawai, *Sci Rep.* **2011**, *1*, 46.

[20] M. L. Perrin, C. A. Martin, F. Prins, A. J. Shaikh, R. Eelkema, J. H. van Esch, J. M. van Ruitenbeek, H. S. J. van der Zant, D. Dulic, *Beilstein J. Nanotechnol.* **2011**, *2*, 714.

[21] Y. Yang, Z. B. Chen, J. Y. Liu, M. Lu, D. Z. Yang, F. Z. Yang, Z. Q. Tian, *Nano Research* **2011**, *4*, 1199.

[22] K. Yoshizawa, *Acc. Chem. Res.* **2012**, *45*, 1612.

[23] S. V. Aradhya, M. Frei, M. S. Hybertsen, L. Venkataraman, *Nat. Mater.* **2012**, *11*, 872.

[24] H. Vazquez, R. Skouta, S. Schneebeli, M. Kamenetska, R. Breslow, L. Venkataraman, M. S. Hybertsen, *Nat. Nanotechnol.* **2012**, *7*, 663.

[25] J. H. Tian, Y. Yang, B. Liu, B. Schollhorn, D. Y. Wu, E. Maisonhaute, A. S. Muns, Y. Chen, C. Amatore, N. J. Tao, Z. Q. Tian, *Nanotechnology* **2010**, *21*, 274012.

[26] X. L. Li, S. Z. Hua, H. D. Chopra, N. J. Tao, *Micro & Nano Letters* **2006**, *1*, 83.

[27] J. M. Baik, S. J. Lee, M. Moskovits, *Nano Lett.* **2009**, *9*, 672.

[28] H. Zhang, C. V. Thompson, F. Stellacci, J. T. L. Thong, *Nanotechnology* **2010**, *21*.

[29] M. Tsutsui, K. Shoji, M. Taniguchi, T. Kawai, *Nano Lett.* **2008**, *8*, 345.

[30] S. L. Johnson, D. P. Hunley, A. Sundararajan, A. T. C. Johnson, D. R. Strachan, *IEEE Tran. Nanotechnol.* **2011**, *10*, 806.

Materials
Views
www.MaterialsViews.com

ADVANCED
MATERIALS
www.advmat.de

REVIEW

[31] J. M. Krans, J. M. Vanruitenbeek, V. V. Fisun, I. K. Yanson, L. J. Dejongh, *Nature* **1995**, *375*, 767.

[32] E. Scheer, N. Agrait, J. C. Cuevas, A. L. Yeyati, B. Ludoph, A. Martin-Rodero, G. R. Bollinger, J. M. van Ruitenbeek, C. Urbina, *Nature* **1998**, *394*, 154.

[33] A. I. Yanson, G. R. Bollinger, H. E. van den Brom, N. Agrait, J. M. van Ruitenbeek, *Nature* **1998**, *395*, 783.

[34] R. H. M. Smit, Y. Noat, C. Untiedt, N. D. Lang, M. C. van Hemert, J. M. van Ruitenbeek, *Nature* **2002**, *419*, 906.

[35] M. A. Reed, C. Zhou, C. J. Muller, T. P. Burgin, J. M. Tour, *Science* **1997**, *278*, 252.

[36] J. J. Parks, A. R. Champagne, T. A. Costi, W. W. Shum, A. N. Pasupathy, E. Neuscamman, S. Flores-Torres, P. S. Cornaglia, A. A. Aligia, C. A. Balseiro, G. K. L. Chan, H. D. Abruna, D. C. Ralph, *Science* **2010**, *328*, 1370.

[37] E. H. Huisman, M. L. Trouwborst, F. L. Bakker, B. de Boer, B. J. van Wees, S. J. van der Molen, *Nano Lett.* **2008**, *8*, 3381.

[38] B. Mann, H. Kuhn, *J. Appl. Phys.* **1971**, *42*, 4398.

[39] M. A. Reed, C. Zhou, M. R. Deshpande, C. J. Muller, T. P. Burgin, L. Jones, J. M. Tour, in, *Molecular Electronics: Science and Technology*, Vol. *852* (Eds: A. Aviram, M. Ratner), **1998**, 133.

[40] W. Y. Wang, T. Lee, I. Kretzschmar, M. A. Reed, *Nano Lett.* **2004**, *4*, 643.

[41] W. Y. Wang, T. Lee, M. A. Reed, *Rep. Prog. Phys.* **2005**, *68*, 523.

[42] H. Song, T. Lee, N. J. Choi, H. Lee, *Appl. Phys. Lett.* **2007**, *91*, 266103.

[43] T. W. Kim, G. N. Wang, H. Lee, T. Lee, *Nanotechnology* **2007**, *18*, 315204.

[44] H. B. Akkerman, P. W. M. Blom, D. M. de Leeuw, B. de Boer, *Nature* **2006**, *441*, 69.

[45] a) H. Haick, D. Cahen, *Acc. Chem. Res.* **2008**, *41*, 359; b) G. L. Fisher, A. V. Walker, A. E. Hooper, T. B. Tighe, K. B. Bahnck, H. T. Skriba, M. D. Reinard, B. C. Haynie, R. L. Opila, N. Winograd, D. L. Allara, *J. Am. Chem. Soc.* **2002**, *124*, 5528.

[46] A. J. Kronemeijer, I. Katsouras, E. H. Huisman, P. A. van Hal, T. C. T. Geuns, P. W. M. Blom, D. M. de Leeuw, *Small* **2011**, *7*, 1593.

[47] G. Wang, S. I. Na, T. W. Kim, Y. Kim, S. Park, T. Lee, *Org. Electron* **2012**, *13*, 771.

[48] a) P. A. Van Hal, E. C. P. Smits, T. C. T. Geuns, H. B. Akkerman, B. C. De Brito, S. Perissinotto, G. Lanzani, A. J. Kronemeijer, V. Geskin, J. Cornil, P. W. M. Blom, B. De Boer, D. M. De Leeuw, *Nat. Nanotechnol.* **2008**, *3*, 749; b) S. Park, G. Wang, B. Cho, Y. Kim, S. Song, Y. Ji, M. H. Yoon, T. Lee, *Nat. Nanotechnol.* **2012**, *7*, 438.

[49] A. P. Bonifas, R. L. McCreery, *Nat. Nanotechnol.* **2010**, *5*, 612.

[50] A. P. Bonifas, R. L. McCreery, *Nano Lett.* **2011**, *11*, 4725.

[51] a) K. Slowinski, R. V. Chamberlain, C. J. Miller, M. Majda, *J. Am. Chem. Soc.* **1997**, *119*, 11910; b) E. Tran, M. A. Rampi, G. M. Whitesides, *Angew. Chem. Int Ed.* **2004**, *43*, 3835.

[52] a) M. L. Chabinyc, X. X. Chen, R. E. Holmlin, H. Jacobs, H. Skulason, C. D. Frisbie, V. Mujica, M. A. Ratner, M. A. Rampi, G. M. Whitesides, *J. Am. Chem. Soc.* **2002**, *124*, 11730; b) F. von Wrochem, D. Q. Gao, F. Scholz, H. G. Nothofer, G. Nelles, J. M. Wessels, *Nat. Nanotechnol.* **2010**, *5*, 618; c) S. Sek, R. Bilewicz, K. Slowinski, *Chem. Commun.* **2004**, *4*, 404; d) E. Tran, C. Grave, G. A. Whitesides, M. A. Rampi, *Electrochim. Acta* **2005**, *50*, 4850.

[53] C. A. Nijhuis, W. F. Reus, J. R. Barber, M. D. Dickey, G. M. Whitesides, *Nano Lett.* **2010**, *10*, 3611.

[54] L. Cademartiri, M. M. Thuo, C. A. Nijhuis, W. F. Reus, S. Tricard, J. R. Barber, R. N. S. Sodhi, P. Brodersen, C. Kim, R. C. Chiechi, G. M. Whitesides, *J. Phys. Chem. C* **2012**, *116*, 10848.

[55] X. F. Guo, J. P. Small, J. E. Klare, Y. L. Wang, M. S. Purewal, I. W. Tam, B. H. Hong, R. Caldwell, L. M. Huang, S. O'Brien, J. M. Yan, R. Breslow, S. J. Wind, J. Hone, P. Kim, C. Nuckolls, *Science* **2006**, *311*, 356.

[56] a) H. Song, Y. Kim, J. Ku, Y. H. Jang, H. Jeong, T. Lee, *Appl. Phys. Lett.*, **2009** *94*; b) A. K. Mahapatro, J. W. Ying, T. Ren, D. B. Janes, *Nano Lett.* **2008**, *8*, 2131.

[57] A. Mangin, A. Anthore, M. L. Della Rocca, E. Boulat, P. Lafarge, *J. Appl. Phys.* **2009**, *105*, 14313.

[58] D. R. Ward, N. J. Halas, J. W. Ciszek, J. M. Tour, Y. Wu, P. Nordlander, D. Natelson, *Nano Lett.* **2008**, *8*, 919.

[59] a) D. R. Strachan, D. E. Johnston, B. S. Guiton, S. S. Datta, P. K. Davies, D. A. Bonnell, A. T. C. Johnson, *Phys. Rev. Lett.* **2008**, *100*; b) B. Gao, E. A. Osorio, K. B. Gaven, H. S. J. van der Zant, *Nanotechnology* **2009**, *20*, 415207.

[60] D. E. Johnston, D. R. Strachan, A. T. C. Johnson, *Nano Lett.* **2007**, *7*, 2774.

[61] D. C. Wei, Y. Q. Liu, L. C. Cao, Y. Wang, H. L. Zhang, G. Yu, *Nano Lett.* **2008**, *8*, 1625.

[62] Y. Lu, B. Goldsmith, D. R. Strachan, J. H. Lim, Z. T. Luo, A. T. C. Johnson, *Small* **2010**, *6*, 2748.

[63] H. Song, Y. Kim, Y. H. Jang, H. Jeong, M. A. Reed, T. Lee, *Nature* **2009**, *462*, 1039.

[64] W. J. Liang, M. P. Shores, M. Bockrath, J. R. Long, H. Park, *Nature* **2002**, *417*, 725.

[65] H. B. Heersche, Z. de Groot, J. A. Folk, H. S. J. van der Zant, C. Romeike, M. R. Wegewijs, L. Zobbi, D. Barreca, E. Tondello, A. Cornia, *Phys. Rev. Lett.* **2006**, *96*, 206801.

[66] C. A. Martin, J. M. van Ruitenbeek, H. S. J. van der Zant, *Nanotechnology* **2010**, *21*, 265201.

[67] H. B. Heersche, Z. de Groot, J. A. Folk, L. P. Kouwenhoven, H. S. J. van der Zant, A. A. Houck, J. Labaziewicz, I. L. Chuang, *Phys. Rev. Lett.* **2006**, *96*, 17205.

[68] a) M. F. Crommie, C. P. Lutz, D. M. Eigler, *Nature* **1993**, *363*, 524; b) J. Repp, G. Meyer, S. M. Stojkovic, A. Gourdon, C. Joachim, *Phys. Rev. Lett.* **2005**, *94*, 26803.

[69] L. Venkataraman, J. E. Klare, C. Nuckolls, M. S. Hybertsen, M. L. Steigerwald, *Nature* **2006**, *442*, 904.

[70] a) B. Q. Xu, N. J. J. Tao, *Science* **2003**, *301*, 1221; b) J. A. Stroscio, D. M. Eigler, *Science* **1991**, *254*, 1319; c) A. Bannani, C. Bobisch, R. Moller, *Science* **2007**, *315*, 1824; d) P. Liljeroth, J. Repp, G. Meyer, *Science* **2007**, *317*, 1203.

[71] L. A. Bumm, J. J. Arnold, M. T. Cygan, T. D. Dunbar, T. P. Burgin, L. Jones, D. L. Allara, J. M. Tour, P. S. Weiss, *Science* **1996**, *271*, 1705.

[72] S. W. Wu, N. Ogawa, W. Ho, *Science* **2006**, *312*, 1362.

[73] a) Z. H. Li, Y. Q. Liu, S. F. L. Mertens, I. V. Pobelov, T. Wandlowski, *J. Am. Chem. Soc.* **2010**, *132*, 8187; b) B. Q. Xu, X. Y. Xiao, X. M. Yang, L. Zang, N. J. Tao, *J. Am. Chem. Soc.* **2005**, *127*, 2386.

[74] a) I. V. Pobelov, Z. H. Li, T. Wandlowski, *J. Am. Chem. Soc.* **2008**, *130*, 16045; b) F. Chen, J. He, C. Nuckolls, T. Roberts, J. E. Klare, S. Lindsay, *Nano Lett.* **2005**, *5*, 503.

[75] a) V. B. Engelkes, J. M. Beebe, C. D. Frisbie, *J. Phys. Chem. B* **2005**, *109*, 16801; b) S. H. Choi, C. Risko, M. C. R. Delgado, B. Kim, J. L. Bredas, C. D. Frisbie, *J. Am. Chem. Soc.* **2010**, *132*, 4358.

[76] G. Wang, T. W. Kim, G. Jo, T. Lee, *J. Am. Chem. Soc.* **2009**, *131*, 5980.

[77] N. J. Tao, *Phys. Rev. Lett.* **1996**, *76*, 4066.

[78] X. D. Cui, A. Primak, X. Zarate, J. Tomfohr, O. F. Sankey, A. L. Moore, T. A. Moore, D. Gust, G. Harris, S. M. Lindsay, *Science* **2001**, *294*, 571.

[79] J. Moreland, J. W. Ekin, *J. Appl. Phys.* **1985**, *58*, 3888.

[80] C. J. Muller, J. M. Vanruitenbeek, L. J. Dejongh, *Physica C* **1992**, *191*, 485.

[81] C. J. Muller, J. M. Vanruitenbeek, L. J. Dejongh, *Phys. Rev. Lett.* **1992**, *69*, 140.

[82] M. M. Jobbins, A. F. Raigoza, S. A. Kandel, *Rev. Sci. Instrum.* **2012**, *83*, 36105.

[83] O. L. Guise, J. W. Ahner, M. C. Jung, P. C. Goughnour, J. T. Yates, *Nano Lett.* **2002**, *2*, 191.

[84] a) B. Liu, J. Xiang, J. H. Tian, C. Zhong, B. W. Mao, F. Z. Yang, Z. B. Chen, S. T. Wu, Z. Q. Tian, *Electrochim. Acta* **2005**, *50*, 3041; b) Y. Yang, J. Y. Liu, Z. B. Chen, J. H. Tian, X. Jin, B. Liu, X. L. Li, Z. Z. Luo, M. Lu, F. Z. Yang, N. J. Tao, Z. Q. Tian, *Nanotechnology* **2011**, *22*, 375131; c) G. Mészáros, S. Kronholz, S. Karthäuser, D. Mayer, T. Wandlowski, *Appl. Phys. A* **2007**, *87*, 569.

[85] Z. W. Yi, M. Banzet, A. Offenhäusser, D. Mayer, *Phys. Status. Solidi RRL* **2010**, *4*, 73.

[86] S. Boussaad, N. J. Tao, *Appl. Phys. Lett.* **2002**, *80*, 2398.

[87] J. Xiang, B. Liu, S. T. Wu, B. Ren, F. Z. Yang, B. W. Mao, Y. L. Chow, Z. Q. Tian, *Angew. Chem. Int Ed.* **2005**, *44*, 1265.

[88] Z. W. Yi, S. Trellenkamp, A. Offenhäusser, D. Mayer, *Chem. Commun.* **2010**, *46*, 8014.

[89] S. P. Liu, S. H. Weisbrod, Z. Tang, A. Marx, E. Scheer, A. Erbe, *Angew. Chem. Int Ed.* **2010**, *49*, 3313.

[90] Y. Kim, T. Pietsch, A. Erbe, W. Belzig, E. Scheer, *Nano Lett.* **2011**, *11*, 3734.

[91] Y. Kim, T. J. Hellmuth, D. Sysoiev, F. Pauly, T. Pietsch, J. Wolf, A. Erbe, T. Huhn, U. Groth, U. E. Steiner, E. Scheer, *Nano Lett.* **2012**, *12*, 3736.

[92] a) E. Lörtscher, H. B. Weber, H. Riel, *Phys. Rev. Lett.* **2007**, *98*, 176807; b) C. Zhou, C. J. Muller, M. R. Deshpande, J. W. Sleight, M. A. Reed, *Appl. Phys. Lett.* **1995**, *67*, 1160; c) S. M. Wu, M. T. González, R. Huber, S. Grunder, M. Mayor, C. Schönenberger, M. Calame, *Nat. Nanotechnol.* **2008**, *3*, 569.

[93] E. Lörtscher, M. Elbing, M. Tschudy, C. von Hanisch, H. B. Weber, M. Mayor, H. Riel, *Chem. Phys. Chem.* **2008**, *9*, 2252.

[94] D. Secker, S. Wagner, S. Ballmann, R. Hartle, M. Thoss, H. B. Weber, *Phys. Rev. Lett.* **2011**, *106*, 136801.

[95] S. Ballmann, R. Hartle, P. B. Coto, M. Elbing, M. Mayor, M. R. Bryce, M. Thoss, H. B. Weber, *Phys. Rev. Lett.* **2012**, *109*, 56801.

[96] R. Huber, M. T. González, S. Wu, M. Langer, S. Grunder, V. Horhoiu, M. Mayor, M. R. Bryce, C. S. Wang, R. Jitchati, C. Schönenberger, M. Calame, *J. Am. Chem. Soc.* **2008**, *130*, 1080.

[97] N. J. Tao, *Nat. Nanotechnol.* **2006**, *1*, 173.

[98] I. Díez-Pérez, J. Hihath, T. Hines, Z. S. Wang, G. Zhou, K. Mullen, N. J. Tao, *Nat. Nanotechnol.* **2011**, *6*, 226.

[99] E. Lörtscher, J. W. Ciszek, J. Tour, H. Riel, *Small* **2006**, *2*, 973.

[100] D. Xiang, Y. Zhang, F. Pyatkov, A. Offenhäusser, D. Mayer, *Chem. Commun.* **2011**, *47*, 4760.

[101] E. Lörtscher, H. Riel, *Chimia* **2010**, *64*, 376.

[102] P. Jarillo-Herrero, *Science* **2010**, *328*, 1362.

[103] A. R. Champagne, A. N. Pasupathy, D. C. Ralph, *Nano Lett.* **2005**, *5*, 305.

[104] a) M. Kiguchi, K. Murakoshi, *Thin Solid Films* **2009**, *518*, 466; b) D. Dulić, S. Tuukkanen, C. L. Chung, A. Isambert, P. Lavie, A. Filoramo, *Nanotechnology* **2009**, *20*, 115502.

[105] X. Y. Xiao, B. Q. Xu, N. J. Tao, *Angew. Chem. Int Ed.* **2004**, *43*, 6148.

[106] D. Xiang, F. Pyatkov, F. Schroper, A. Offenhäusser, Y. Zhang, D. Mayer, *Chem. Eur. J.* **2011**, *17*, 13166.

[107] a) M. Kiguchi, S. Nakashima, T. Tada, S. Watanabe, S. Tsuda, Y. Tsuji, J. Terao, *Small* **2012**, *8*, 726; b) A. J. Simbeck, G. G. Qian, S. K. Nayak, G. C. Wang, K. M. Lewis, *Surf. Sci.* **2012**, *606*, 1412.

[108] M. T. González, S. M. Wu, R. Huber, S. J. van der Molen, C. Schönenberger, M. Calame, *Nano Lett.* **2006**, *6*, 2238.

[109] W. J. Hong, H. Valkenier, G. Meszaros, D. Z. Manrique, A. Mishchenko, A. Putz, P. M. Garcia, C. J. Lambert, J. C. Hummelen, T. Wandlowski, *Beilstein J. Nanotechnol.* **2011**, *2*, 699.

[110] M. G. Reuter, M. C. Hersam, T. Seideman, M. A. Ratner, *Nano Lett.* **2012**, *12*, 2243.

[111] P. Makk, D. Tomaszewski, J. Martinek, Z. Balogh, S. Csonka, M. Wawrzyniak, M. Frei, L. Venkataraman, A. Halbritter, *ACS Nano* **2012**, *6*, 3411.

[112] D. Natelson, *ACS Nano* **2012**, *6*, 2871.

[113] L. Grüter, M. T. González, R. Huber, M. Calame, C. Schönenberger, *Small* **2005**, *1*, 1067.

[114] L. Grüter, F. Y. Cheng, T. T. Heikkila, M. T. González, F. O. Diederich, C. Schönenberger, M. Calame, *Nanotechnology* **2005**, *16*, 2143.

[115] Y. Q. Xu, C. F. Fang, B. Cui, G. M. Ji, Y. X. Zhai, D. S. Liu, *Appl. Phys. Lett.* **2011**, *99*, 043304.

[116] a) R. Vincent, S. Klyatskaya, M. Ruben, W. Wernsdorfer, F. Balestro, *Nature* **2012**, *488*, 357; b) I. W. P. Chen, M. D. Fu, W. H. Tseng, J. Y. Yu, S. H. Wu, C. J. Ku, C. H. Chen, S. M. Peng, *Angew. Chem. Int Ed.* **2006**, *45*, 5814.

[117] L. Luo, A. Benameur, P. Brignou, S. H. Choi, S. Rigaut, C. D. Frisbie, *J. Phys. Chem. C* **2011**, *115*, 19955.

[118] J. Heurich, J. C. Cuevas, W. Wenzel, G. Schon, *Phys. Rev. Lett.* **2002**, *88*, 256803.

[119] K. Yoshizawa, T. Tada, A. Staykov, *J. Am. Chem. Soc.* **2008**, *130*, 9406.

[120] a) Z. J. Donhauser, B. A. Mantooth, K. F. Kelly, L. A. Bumm, J. D. Monnell, J. J. Stapleton, D. W. Price, A. M. Rawlett, D. L. Allara, J. M. Tour, P. S. Weiss, *Science* **2001**, *292*, 2303; b) M. Rahimi, A. Troisi, *Phys. Rev. B* **2009**, *79*, 113413; c) W. Auwarter, K. Seufert, F. Bischoff, D. Ecija, S. Vijayaraghavan, S. Joshi, F. Klappenberger, N. Samudrala, J. V. Barth, *Nat. Nanotechnol.* **2012**, *7*, 41.

[121] a) D. R. Fruge, G. D. Fong, F. K. Fong, *J. Am. Chem. Soc.* **1979**, *101*, 3694; b) I. Gerhardt, L. J. Mai, A. Lamas-Linares, C. Kurtsiefer, *Sensors* **2011**, *11*, 905; c) C. Raduge, G. Papastavrou, D. G. Kurth, H. Motschmann, *Eur. Phys. J. E* **2003**, *10*, 103.

[122] D. Dulic, S. J. van der Molen, T. Kudernac, H. T. Jonkman, J. J. D. de Jong, T. N. Bowden, J. van Esch, B. L. Feringa, B. J. van Wees, *Phys. Rev. Lett.* **2003**, *91*.

[123] A. J. Kronemeijer, H. B. Akkerman, T. Kudernac, B. J. van Wees, B. L. Feringa, P. W. M. Blom, B. de Boer, *Adv. Mater.* **2008**, *20*, 1467.

[124] a) E. Flaxer, O. Sneh, O. Cheshnovsky, *Science* **1993**, *262*, 2012; b) X. H. Qiu, G. V. Nazin, W. Ho, *Science* **2003**, *299*, 542.

[125] A. Aviram, M. A. Ratner, *Chem. Phys. Lett.* **1974**, *29*, 277.

[126] P. E. Kornilovitch, A. M. Bratkovsky, R. S. Williams, *Phys. Rev. B* **2002**, *66*.

[127] a) P. Damle, T. Rakshit, M. Paulsson, S. Datta, *Ieee Transactions on Nanotechnology* **2002**, *1*, 145; b) F. Zahid, A. W. Ghosh, M. Paulsson, E. Polizzi, S. Datta, *Phys. Rev. B* **2004**, *70*.

[128] S. Datta, W. D. Tian, S. H. Hong, R. Reifenberger, J. I. Henderson, C. P. Kubiak, *Phys. Rev. Lett.* **1997**, *79*, 2530.

[129] M. Elbing, R. Ochs, M. Koentopp, M. Fischer, C. von Hanisch, F. Weigend, F. Evers, H. B. Weber, M. Mayor, *Proc. Natl. Acad. Sci. U. S. A.* **2005**, *102*, 8815.

[130] R. A. Kiehl, J. D. Le, P. Candra, R. C. Hoye, T. R. Hoye, *Appl. Phys. Lett.* **2006**, *88*, 172102.

[131] N. Kang, A. Erbe, E. Scheer, *Appl. Phys. Lett.* **2010**, *96*, 023701.

[132] P. W. Anderson, *Physical Review* **1961**, *124*, 41.

[133] G. D. Scott, D. Natelson, *ACS Nano* **2010**, *4*, 3560.

[134] E. A. Osorio, K. Moth-Poulsen, H. S. J. van der Zant, J. Paaske, P. Hedegard, K. Flensberg, J. Bendix, T. Bjørnholm, *Nano Lett.* **2010**, *10*, 105.

[135] a) W. Haiss, C. S. Wang, I. Grace, A. S. Batsanov, D. J. Schiffrin, S. J. Higgins, M. R. Bryce, C. J. Lambert, R. J. Nichols, *Nat. Mater.* **2006**, *5*, 995; b) W. T. Geng, J. Nara, T. Ohno, *Appl. Phys. Lett.* **2004**, *85*, 5992.

[136] K. Moth-Poulsen, Bjørnholm, *Nat. Nanotechnol.* **2009**, *4*, 551.

[137] A. Danilov, S. Kubatkin, S. Kafanov, P. Hedegard, N. Stuhr-Hansen, K. Moth-Poulsen, T. Bjørnholm, *Nano Lett.* **2008**, *8*, 1.

[138] J. M. Beebe, B. Kim, J. W. Gadzuk, C. D. Frisbie, J. G. Kushmerick, *Phys. Rev. Lett.* **2006**, *97*, 026801.

[139] E. H. Huisman, C. M. Guedon, B. J. van Wees, S. J. van der Molen, *Nano Lett.* **2009**, *9*, 3909.

Materials
Views
www.MaterialsViews.com

ADVANCED
MATERIALS
www.advmat.de

REVIEW

[140] F. Mirjani, J. M. Thijssen, S. J. van der Molen, *Phys. Rev. B* **2011**, *84*, 115402.

[141] M. L. Trouwborst, C. A. Martin, R. H. M. Smit, C. M. Guedon, T. A. Baart, S. J. van der Molen, J. M. van Ruitenbeek, *Nano Lett.* **2011**, *11*, 614.

[142] H. Basch, M. A. Ratner, *J. Chem. Phys.* **2004**, *120*, 5761.

[143] C. Bruot, J. Hihath, N. J. Tao, *Nat. Nanotechnol.* **2012**, *7*, 35.

[144] C. M. Guedon, H. Valkenier, T. Markussen, K. S. Thygesen, J. C. Hummelen, S. J. van der Molen, *Nat. Nanotechnol.* **2012**, *7*, 304.

[145] G. C. Solomon, D. Q. Andrews, T. Hansen, R. H. Goldsmith, M. R. Wasielewski, R. P. Van Duyne, M. A. Ratner, *J. Chem. Phys.* **2008**, *129*, 54701.

[146] R. Hartle, M. Butzin, O. Rubio-Pons, M. Thoss, *Phys. Rev. Lett.* **2011**, *107*, 046802.

[147] H. Park, J. Park, A. K. L. Lim, E. H. Anderson, A. P. Alivisatos, P. L. McEuen, *Nature* **2000**, *407*, 57.

[148] a) S. Kubatkin, A. Danilov, M. Hjort, J. Cornil, J. L. Bredas, N. Stuhr-Hansen, P. Hedegard, T. Bjørnholm, *Nature* **2003**, *425*, 698; b) J. Park, A. N. Pasupathy, J. I. Goldsmith, C. Chang, Y. Yaish, J. R. Petta, M. Rinkoski, J. P. Sethna, H. D. Abruna, P. L. McEuen, D. C. Ralph, *Nature* **2002**, *417*, 722; c) L. H. Yu, Z. K. Keane, J. W. Ciszek, L. Cheng, J. M. Tour, T. Baruah, M. R. Pederson, D. Natelson, *Phys. Rev. Lett.* **2005**, *95*, 256803; d) L. H. Yu, D. Natelson, *Nano Lett.* **2004**, *4*, 79.

[149] Y. Q. Xue, M. A. Ratner, *Phys. Rev. B* **2003**, *68*, 115406.

[150] J. R. Petta, S. K. Slater, D. C. Ralph, *Phys. Rev. Lett.* **2004**, *93*, 136601.

[151] R. Yamada, M. Noguchi, H. Tada, *Appl. Phys. Lett.* **2011**, *98*, 53110.

[152] E. Y. Tsymbal, A. Sokolov, I. F. Sabirianov, B. Doudin, *Phys. Rev. Lett.* **2003**, *90*, 186602.

[153] J. J. Parks, A. R. Champagne, G. R. Hutchison, S. Flores-Torres, H. D. Abruna, D. C. Ralph, *Phys. Rev. Lett.* **2007**, *99*, 26601.

[154] H. Ohnishi, Y. Kondo, K. Takayanagi, *Nature* **1998**, *395*, 780.

[155] V. Rodrigues, J. Bettini, A. R. Rocha, L. G. C. Rego, D. Ugarte, *Phys. Rev. B* **2002**, *65*, 153402.

[156] V. Rodrigues, D. Ugarte, *Nanotechnology* **2002**, *13*, 404.

[157] M. Lagos, V. Rodrigues, D. Ugarte, *J. Electron Spectrosc. Relat. Phenom.* **2007**, *156*, 20.

[158] M. J. Lagos, P. A. S. Autreto, D. S. Galvao, D. Ugarte, *J. Appl. Phys.* **2012**, *111*, 124316.

[159] J. H. Tian, B. Liu, X. L. Li, Z. L. Yang, B. Ren, S. T. Wu, N. J. Tao, Z. Q. Tian, *J. Am. Chem. Soc.* **2006**, *128*, 14748.

[160] M. Tsutsui, M. Taniguchi, *Sensors* **2012**, *12*, 7259.

[161] J. Fock, J. K. Sorensen, E. Lörtscher, T. Vosch, C. A. Martin, H. Riel, K. Kilsa, T. Bjørnholm, H. van der Zant, *Phys. Chem. Chem. Phys.* **2011**, *13*, 14325.

[162] a) M. Taniguchi, M. Tsutsui, K. Yokota, T. Kawai, *Nanotechnology* **2009**, *20*; b) M. Tsutsui, M. Taniguchi, K. Shoji, K. Yokota, T. Kawai, *Nanoscale* **2009**, *1*, 164.

[163] Y. Kim, H. Song, F. Strigl, H. F. Pernau, T. Lee, E. Scheer, *Phys. Rev. Lett.* **2011**, *106*, 196804.

[164] Y. Kim, H. Song, D. Kim, T. Lee, H. Jeong, *ACS Nano* **2010**, *4*, 4426.

[165] Z. M. Wu, S. M. Wu, S. Oberholzer, M. Steinacher, M. Calame, C. Schönenberger, *Phys. Rev. B* **2008**, *78*, 235421.

[166] R. Ochs, D. Secker, M. Elbing, M. Mayor, H. B. Weber, *Faraday Discuss.* **2006**, *131*, 281.

[167] V. A. Sydoruk, D. Xiang, S. A. Vitusevich, M. V. Petrychuk, A. Vladyka, Y. Zhang, A. Offenhäusser, V. A. Kochelap, A. E. Belyaev, D. Mayer, *J. Appl. Phys.* **2012**, *112*, 14908.

[168] D. Seeker, H. B. Weber, *Phys. Status Solidi B* **2007**, *244*, 4176.

[169] J. Koch, F. von Oppen, *Phys. Rev. Lett.* **2005**, *94*, 206804.

[170] M. Tsutsui, M. Taniguchi, T. Kawai, *Nat. Commun.* **2010**, *1*, 138.

[171] D. Djukic, J. M. van Ruitenbeek, *Nano Lett.* **2006**, *6*, 789.

[172] P. J. Wheeler, J. N. Russom, K. Evans, N. S. King, D. Natelson, *Nano Lett.* **2010**, *10*, 1287.

[173] a) L. Olesen, E. Laegsgaard, I. Stensgaard, F. Besenbacher, J. Schiøtz, P. Stoltze, K. W. Jacobsen, J. K. Nørskov, *Phys. Rev. Lett.* **1994**, *72*, 2251; b) L. Olesen, E. Laegsgaard, I. Stensgaard, F. Besenbacher, J. Schiotz, P. Stoltze, K. W. Jacobsen, J. K. Norskov, *Phys. Rev. Lett.* **1995**, *74*, 2147; c) Y. Kurui, Y. Oshima, M. Okamoto, K. Takayanagi, *Phys. Rev. B* **2008**, *77*, 161403.

[174] J. M. Krans, C. J. Muller, N. Vanderpost, F. R. Postma, A. P. Sutton, T. N. Todorov, J. M. Vanruitenbeek, *Phys. Rev. Lett.* **1995**, *74*, 2146.

[175] a) N. Agrait, A. L. Yeyati, J. M. van Ruitenbeek, *Phys. Rep.* **2003**, *377*, 81; b) M. Dreher, F. Pauly, J. Heurich, J. C. Cuevas, E. Scheer, P. Nielaba, *Phys. Rev. B* **2005**, *72*, 075435.

[176] C. A. Martin, R. H. M. Smit, H. S. J. van der Zant, J. M. van Ruitenbeek, *Nano Lett.* **2009**, *9*, 2940.

[177] F. Prins, T. Hayashi, B. van Steenwijk, B. Gao, E. A. Osorio, K. Muraki, H. S. J. van der Zant, *Appl. Phys. Lett.* **2009**, *94*, 123108.

[178] M. Muller, R. Montbrun, M. Marz, V. Fritsch, C. Surgers, H. von Lohneysen, *Nano Lett.* **2011**, *11*, 574.

[179] M. Tsutsui, M. Taniguchi, T. Kawai, *Nano Lett.* **2009**, *9*, 1659.

[180] C. A. Martin, R. H. M. Smit, R. van Egmond, H. S. J. van der Zant, J. M. van Ruitenbeek, *Rev. Sci. Instrum.* **2011**, *82*, 53907.

[181] S. Y. Guo, J. Hihath, N. J. Tao, *Nano Lett.* **2011**, *11*, 927.

[182] R. Waitz, O. Schecker, E. Scheer, *Rev. Sci. Instrum.* **2008**, *79*, 093901.

[183] D. K. James, J. M. Tour, *Chem. Mater.* **2004**, *16*, 4423.

[184] a) Z. L. Cheng, R. Skouta, H. Vazquez, J. R. Widawsky, S. Schneebeli, W. Chen, M. S. Hybertsen, R. Breslow, L. Venkataraman, *Nat. Nanotechnol.* **2011**, *6*, 353; b) A. Vilan, O. Yaffe, A. Biller, A. Salomon, A. Kahn, D. Cahen, *Adv. Mater.* **2010**, *22*, 140.

[185] a) L. H. Yu, N. Gergel-Hackett, C. D. Zangmeister, C. A. Hacker, C. A. Richter, J. G. Kushmerick, *J. Phys. Condens. Matter* **2008**, *20*, 374114; b) M. Coll, L. H. Miller, L. J. Richter, D. R. Hines, O. D. Jurchescu, N. Gergel-Hackett, C. A. Richter, C. A. Hacker, *J. Am. Chem. Soc.* **2009**, *131*, 12451.

[186] M. Tsutsui, Y. Taninouchi, S. Kurokawa, A. Sakai, *J. Appl. Phys.* **2006**, *100*, 94302.

[187] G. Jo, M. Choe, S. Lee, W. Park, Y. H. Kahng, T. Lee, *Nanotechnology* **2012**, *23*, 75702.

[188] a) M. Tsutsui, M. Taniguchi, T. Kawai, *Nano Lett.* **2008**, *8*, 3293; b) Z. F. Huang, B. Q. Xu, Y. C. Chen, M. Di Ventra, N. J. Tao, *Nano Lett.* **2006**, *6*, 1240.

[189] N. A. Zimbovskaya, M. R. Pederson, *Phys. Rep. Rev. Sec. Phys. Lett.* **2011**, *509*, 1.

[190] D. X. Wang, J. W. Zhao, S. Hu, X. Yin, S. Liang, Y. H. Liu, S. Y. Deng, *Nano Lett.* **2007**, *7*, 1208.

[191] L. L. Lin, C. K. Wang, Y. Luo, *ACS Nano* **2011**, *5*, 2257.

[192] a) J. P. Bergfield, C. A. Stafford, *Phys. Rev. B* **2009**, *79*, 245125; b) A. Saffarzadeh, *J. Appl. Phys.* **2008**, *103*, 083705; c) A. Troisi, M. A. Ratner, *Nano Lett.* **2006**, *6*, 1784; d) T. A. Papadopoulos, I. M. Grace, C. J. Lambert, *Phys. Rev. B* **2006**, *74*, 193306; e) C. C. Kaun, R. Jorn, T. Seideman, *Phys. Rev. B* **2006**, *74*, 045415.

[193] J. M. van Ruitenbeek, *Beilstein J. Nanotechnol.* **2011**, *2*, 691.